IDB Inter-American Development Bank

IDB WORKING PAPER SERIES Nº IDB-WP-01384

The Impact of Sargassum: Evidence from the Mexican Coast

Maja Schling
Roberto Guerrero Compeán
Nicolás Pazos
Allison Bailey
Katie Arkema
Mary Ruckelshaus

Inter-American Development Bank
Environment, Rural Development and Disaster Risk Management Division

September 2022

The Impact of Sargassum: Evidence from the Mexican Coast

Maja Schling
Roberto Guerrero Compeán
Nicolás Pazos
Allison Bailey
Katie Arkema
Mary Ruckelshaus

Inter-American Development Bank
Environment, Rural Development and Disaster Risk Management Division

September 2022

Cataloging-in-Publication data provided by the
Inter-American Development Bank
Felipe Herrera Library
The economic impact of Sargassum: evidence from the mexican coast / Maja Schling, Roberto Guerrero Compeán, Nicolás Pazos, Allison Bailey, Katie Arkema, Mary Ruckelshaus.
p. cm. — (IDB Working Paper Series ; 1384)
Includes bibliographic references.
1. Sargassum-Economic aspects-Mexico. 2. Coastal zone management-Mexico. 3. Geographic information systems-Mexico. I. Schling, Maja. II. Guerrero Compeán, Roberto. III. Pazos, Nicolás. IV. Bailey, Allison. V. Arkema, Katie. VI. Ruckelshaus, Mary. VII. Inter-American Development Bank. Environment, Rural Development and Risk Management Division. VIII. Series
IDB-WP-1384

JEL Codes: C23, C52, N56, O44, Q56, R11 Z32

Keywords: Sargassum, economic growth, nighttime lights data, coastal zone management, Mexico

http://www.iadb.org

The Economic Impact of Sargassum: Evidence from the Mexican Coast

Maja Schling[†], *Roberto Guerrero Compeán*[‡], *Nicolás Pazos*[§], *Allison Bailey*[¤], *Katie Arkema*[¬], *Mary Ruckelshaus*[**]

September 2022

Abstract

This paper assesses the local economic impact of pelagic Sargassum seaweed washed ashore in tourism-heavy coastal zones in the Mexican State of Quintana Roo. The study relies on a carefully designed geographic information systems (GIS) dataset of monthly observations from 2016 to 2019 for 157 beach segments. The dataset comprises an innovate measure of Sargassum seaweed presence, remotely sensed nighttime light intensity as a proxy of economic growth, as well as information on key infrastructure, sociodemographic and beach characteristics. We apply a fixed-effects regression model that controls for general time trends and unobserved, time-invariant differences across observations. We estimate that the presence of Sargassum in a beach segment reduces nighttime light intensity by 17.5%, representing an approximate 11.6% decrease in gross local product. Considering that impacts of Sargassum on local economic activity may be delayed due to reputational effects, our analysis finds that significant lagged effects can be detected up until 12 months after Sargassum was detected on the shoreline. These effect sizes range between a 5.9 and a 9.9% reduction in gross local product. Various robustness checks, including an adjusted measurement of Sargassum and the consideration of potential spatial correlation across beach segments, indicate that estimated impacts are consistently significant and negative across numerous specifications. For one of most tourism-dependent regions in the world, the recurrent influx is one of the most threatening manifestations of climate change. Our research is the first to robustly quantify the economic impact of Sargassum, and highlights the extent to which economic activity is negatively affected by the accumulation of seaweed and how these effects persist over time. The next important step is for both public and private sectors to invest in forecasting systems and containment strategies as well as engage in cleanup efforts to mitigate severe accumulations, inducing economic resilience in coastal communities.

JEL Codes: C23; C52; N56; O44; Q56; R11; Z32

Key Words: Sargassum, economic growth, nighttime lights data, coastal zone management, Mexico

[†] majas@iadb.org, Inter-American Development Bank
[‡] rguerrero@iadb.org, Inter-American Development Bank
[§] nicolaspa@iadb.org, Inter-American Development Bank
[¤] allison.bailey@stanford.edu, Stanford University
[¬] katiearkema@gmail.com, Pacific Northwest National Laboratory
[**] mary.ruckelshaus@stanford.edu, Stanford University

Acknowledgements

The authors would like to thank Borja Reguero and Valeria Chávez Cerón for supporting data collection efforts and providing region-specific knowledge as well as general feedback on the research. The authors are grateful for the feedback received from Alexei Abrahams, Esteban Amaro, Matias Cattaneo, Luis Espinosa Carrasco, Juan Li and Nathan Torbick during the research kickoff seminar held in December 2020. We also thank Rosa Rodríguez Martínez for supporting data collection efforts on Sargassum volumes and cleanup efforts on local Quintana Roo beaches. We are grateful for the contributions by Andre Joseph-Witzig, who provided important input from the InVEST CV model. Lastly, we thank Allen Blackman for his guidance throughout this research project.

1 Introduction

Latin America and the Caribbean has a wealth of coastal natural capital, including over 64,000 km of coastline, that hosts a high concentration of urban areas, and is a hotspot of economic activity (Maldonado et al., 2020). It is estimated that over 23 million people in the Caribbean and the Americas live within 10 meters of the coastline (ibid). Coastal areas are inextricably linked to the Region's recent growth in both GDP and population, as coastal ecosystems support economies and communities with important goods and services, such as fisheries, tourism, and raw materials (Schueler, 2017). Mexico particularly hosts a high concentration of urban areas along its over 12,000 km of coastline, where over 30 million people are estimated to live (CONABIO, 2019). León (2004) in his economic assessment of the Mexican coast estimates that approximately 3.7% of Mexico's GDP comes from economic activities that take place on its coast.

In 2011, pelagic Sargassum began washing ashore along the Caribbean and Gulf of Mexico coastlines in unprecedented quantities, covering whole beaches with seaweed and directly affecting businesses and local communities reliant on tourism and other economic activity within the region's popular coastal zone. Since then, Sargassum blooms have been a common occurrence on the region's shorelines. 2018 saw the first year-round occurrence of Sargassum in the Caribbean Sea (Burrowes et al., 2019). One of the regions hardest hit by these Sargassum blooms is Quintana Roo, one of the main engines of the Mexican coastal economy and Mexico's easternmost state, located in the Yucatán Peninsula. Along its 920 kms of coastline, lies the economic center of Cancún, as well as the towns of Playa del Carmen and Tulum, the ports of Cozumel and Isla Mujeres, and the Riviera Maya district. Their sandy beaches attracted more than 15 million tourists in 2019, generating more than USD 16 billion in revenue and capturing over 43% of Mexico's foreign exchange earnings from tourism (Ministry of Tourism of Quintana Roo, 2019). Tourism is Quintana Roo's most important economic activity, accounting for more than one fifth of the state's GDP as of 2019 (INEGI, 2019). 2018 saw the first year-round occurrence of Sargassum in the Caribbean Sea (Burrowes et al., 2019), and over half a million tons of Sargassum suffocated the coast of Quintana Roo during that period (Robledo & Vázquez-Delfín 2019).

The suspected causes of this algae bloom vary, but a commonly identified trigger is increasingly high nutrient loads flushed out to sea from agriculture and poor land-use in both the Amazon and Congo River Basins and the Mississippi River. In addition, increased iron and phosphate from Saharan dust fall over the mid-Atlantic has also been suggested as a possible cause (Huffard et al, 2014; Amaral-Zettler et al., 2016; Smetacek & Zingone, 2013; Johnson et al, 2013). The explosion of Sargassum blooms have also been linked to global climate change and warmer oceans, where higher than normal temperatures are conducive to algae growth (Louime et al., 2017, Wang et al., 2019). Even though the economic impact of Sargassum blooms has been assessed only anecdotally, there is a large literature on the economic impact of climate change and natural resource shocks. Relying on methods and data by Deschênes and Greenstone (2007), Fisher et al. (2012) use agricultural output and random weather fluctuations information and conclude that predictions for climate-change economic impacts are negative in all but one specification. Similarly, using spatial econometric panel techniques, Felbermayr et al. (2022) show that weather anomalies reduce local income growth. Guerrero Compeán (2013) demonstrates that severe weather conditions lead to sharp declines in consumption and welfare outcomes, particularly among the poor. Tol (2020) reviews 27 published estimates of the economic impact of climate change and argues that that a global mean temperature increase of 2.5 degrees Celsius would make the average person feel as if they had lost 1.3 percent of their income and that the relative economic impact of climate change decline as per capita income rises. In agreement, Maddison and Rehdanz (2011) indicate that poorer and hotter countries are more vulnerable to climate change. Porter et al. (2014) find that climate change reduces agricultural yields by up to 50%, while Dell, Jones and Olken (2009) and Hallegatte (2005) provide evidence that climate change also affects the growth rate of the economy.

While anecdotal evidence (Louime et al., 2017; Ramlogan et al., 2017; Schell et al., 2015; Solarin et al., 2014) suggests that these unprecedented Sargassum events have led not only to a decline in economic revenue, but also to immediate problems for the fishery, transportation and tourism industries of coastal economies, not to mention serious ecological impacts, no rigorous analysis has yet been undertaken to quantify the causal effect on economic activity. Efforts have so far focused on quantifying the frequency and volume of Sargassum influx along the Caribbean coast (e.g. Putman et al, 2018; Wang et al, 2019; Wang & Hu, 2017) and identifying the origin and triggers of algae bloom (e.g. Gower et al., 2013; Oviatt et al., 2019; Cabanillas-Terán et al., 2019) and its ecosystemic effects (van Tussenbroek et al., 2017). To date, evidence on the environmental and economic impacts of Sargassum is largely of qualitative nature. For instance, a study by FAO (2017) points to the negative effects on inshore fish nurseries, while Gavio and Santos-Martinez (2018) documented the reduced chance of turtle hatchlings successfully reaching open ocean. Ramlogan, McConney and Oxenford (2017) document impacts of Sargassum abundance on the fishery value chain, including equipment damage, disruptions in operations and changes in disposable income and productivity. Sargassum blooms have also created a vast raft straddling, slowing down transatlantic navigation significantly (UNEP-CEP, 2021). It has also been reported that decomposing Sargassum causes corrosion of electrical appliances and equipment along the shoreline (Méndez Tejeda & Rosado Jiménez, 2019).

However, given the methodological challenges of identifying a counterfactual state in which Sargassum would not have been present along the coastline, causal estimation of the seaweed's impact on economic activity has not been carried out to date. Furthermore, even though countries have undertaken massive cleaning efforts to combat the negative economic and environmental effects of Sargassum, little information is available on the cost-effectiveness of these solutions. The tourism industry is concerned about Sargassum's negative aesthetic effects on beaches (Burrowes et al., 2019), in addition to the cost of beach cleaning, sometimes borne directly by hotels and businesses along the coast (Rodríguez Martínez et al., 2016). The potential cost of cleaning up the Sargassum inundations across the Caribbean has been estimated to exceed $120 million annually (Milledge and Harvey, 2016), yet it is difficult to justify the large expenditure of public funds without empirical evidence that can support the effectiveness of such investments.

To fill this research gap, we assess the economic impact of Sargassum on economic activity in this region, using novel measurement tools of both Sargassum presence and local economic activity. To do so, we compile a comprehensive GIS dataset of over 157 beach sites in Quintana Roo, Mexico that contains four years of satellite imagery, from 2016 to 2019, using innovative data collection techniques to measure seasonal influx of Sargassum seaweed, and nighttime light intensity data as a proxy of economic growth. To estimate a causal effect of Sargassum presence on economic activity at the beach level, we use a fixed-effects regression model that controls for general time trends and unobserved, time-invariant differences across observations. The methodology further allows us to control for spatial and temporal intercorrelation across adjacent beach sites. Our findings suggest that the presence of Sargassum has a negative effect on local economic activity. We also find these impacts to be long-lasting, as the negative impacts on beach level nighttime light intensity can be observed even after a year of Sargassum detection. This is critical knowledge as governments and the private sector have become increasingly concerned about the adverse effects of Sargassum on tourism-dependent zones as well as the high cost of removal for local authorities and numerous environmental problems. Understanding the magnitude of adverse economic consequences of Sargassum presence can inform the decision-making of stakeholders in terms of directing funding to support Sargassum removal where economic impact might be most severe.

In the next section, we examine the economic importance of coastal zones and present a general characterization of the Mexican Caribbean. We discuss how economic development started in Quintana Roo, as well as its transition from a coastal economy based on small-scale fisheries to a globally recognized tourist destination and preeminent contributor to the country's economic growth. We then describe the issue of increasing influx of pelagic Sargassum along the Caribbean and Gulf of Mexico coastlines, its origin and potential consequences, particularly on the Quintana Roo coastline. Its heavy reliance on beach tourism and recurrent Sargassum events make it an appropriate study area. We then proceed to describe the data and our empirical approach to assess the impact of Sargassum on economic activity. Next, we discuss our main results and carry out a number of robustness checks. Finally, the last section of this paper summarizes our findings and concluding remarks.

1.1 The economic importance of coastal zones

The coast is a critical component of most economies, including Mexico and, more specifically, Quintana Roo. The state's coastal zone and resources represent strategic assets, and many of its communities vigorously seek private investments in coastal tourism and maritime transport, viewing them as offering promising opportunities for the diversification and integration of their economies. Coastal communities are rapidly expanding in response to growth in these sectors as well as urbanization and the intensification of transportation networks along coastal corridors in the Yucatán Peninsula.

Nearly 1.9 million people live in Quintana Roo (INEGI, 2020). Azuz-Adeath and Rivera (2019) estimate that more than 1.4 million (approximately 78%) of the state's inhabitants live in coastal municipalities. Annualized population growth in Quintana Roo's most populated coastal municipalities between 2000 and 2015 was 3.9%, higher than the state's rate of 3.7%, and substantially above the national rate of 1.4% (INEGI 2015). Consequently, as Quintana Roo grows, it is also becoming more coastal. The concentration of people in coastal areas is accompanied by a similarly disproportionate share of the state's economic activity, most of which is coastal dependent and requires a site on, or close to, the coastline. In fact, Torres and Momsen (2005) assess that almost 90% of the state's gross product is generated in coastal zones.

The state's economic base has dramatically evolved over the past forty years. Fishing and other primary activities made up 2% of the Quintana Roo's economy in 1980, and has declined to 0.7% of the gross state product in 2019. The role of manufacturing has also shrunk, from 17% of the state's economic output in 1980 to 11% in 2019. During the same period, however, the participation of the service sector, which tends to generate more marginal GDP growth, increased from 81% to 88%. In particular, tourism alone accounts for roughly half of the state's economy, which explains the state's accelerated rate of economic growth, from 1.9% in the 1980s to 4.6% in the 2010s. Overall, Quintana Roo's gross product has more than quadrupled in forty years, from 67 billion Mexican pesos of 2013 in 1980 to 290 billion in 2019 (INEGI, 2021). Ocean uses and maritime access have been at the heart of Quintana Roo's economic development. Fishing focuses on the capture of species of high commercial value, such as lobster, octopus and shrimp. Fisheries provide employment to approximately 2,000 fishermen, of which more than 90% are in the small-scale sector (CONAPESCA, 2012).

The coast of Quintana Roo also serves as an important node in the flow of goods. The volume of cargo handled in the port of Puerto Morelos amounted to over 21,900 metric tons in 2020. Total tonnage pre-pandemic levels doubled this volume (APIQROO, 2021), having increased gradually over the past 20 years, with indications that port activity in the state is accelerating again in 2021. In addition to coastal and deep-sea shipping, Cozumel, Playa del Carmen, Isla Mujeres, Punta Sam and

Chetumal are recognized as ports for tourists, accounting for more than 14.3 million passengers in 2019 (idem).

Because of its white sand beaches and turquoise blue sea, Quintana Roo is also one of the most important tourist destinations in Latin America and the Caribbean. Tourism is central to the Quintana Roo economy, with more of the state's workers employed by the tourist sector than in any other. With over 50% of the state's workforce dedicated to touristic activities and almost 60% of the state's gross product being generated by tourism, Quintana Roo is the most tourism-dependent state of the nation (Ministry of Tourism of Mexico, 2020), while Cancún is considered the most tourism-dependent urban area in the world (WTTC, 2018). This is the direct result of the Mexican government's involvement in the creation of Cancún as a new tourist resort destination, developing its airport, water systems, energy and tourist infrastructure, as well as the revitalization of archeological sites, in what was in the 1970s one of the poorest and most isolated areas of Mexico. The provision of this infrastructure was primarily financed by the Inter-American Development Bank and occurred in the context of Mexico's regional development goal of initiating and overseeing its tourism industry (IDB, 1972; Bennett & Sharpe, 1985; Clancy, 2001).

1.2 The surge of Sargassum in the Mexican Caribbean and its impact

Sargassum belongs to the group of brown algae (Phaeophyceae) that inhabit the oceans of the world. The pelagic Sargassum subgroup, that is, the one that floats freely in the ocean, is made up of two species: *Sargassum natans* and *Sargassum fluitans*, the former being the most abundant in the Atlantic Ocean. Sargassum exhibits optimal growth at temperatures between 24° and 30° C, and under adequate light, salinity, and temperature conditions, it can duplicate its mass in less than two weeks (Hanisak & Samuel, 1987).

Sargassum naturally reaches all tropical and semi-temperate beaches in the Atlantic Ocean, with seasonal variations caused by regional and local atmospheric and oceanographic conditions. The natural presence of Sargassum on the coast is a source for shelter, food and nutrients in coastal ecosystems, as it provides habitat and direct resources to intertidal organisms, which are essential for bird life. Similarly, decomposing Sargassum is incorporated into coastal sediments, providing nutrients for dune vegetation, which in turn promotes beach stabilization and prevents coastal erosion (Williams & Feagin, 2010).

Since the summer of 2011, substantially large volumes of Sargassum have recurrently washed ashore along the coastlines of the Caribbean, West Africa and northeastern Brazil (Franks et al., 2016; Wang et al., 2019). Gower, Young and King (2013) report widespread Sargassum lines being captured by color satellite, with numerous beach stranding events across the North Atlantic. Accumulations of Sargassum in the Mexican Caribbean have continued for several years now (Chávez et al., 2014). The 2015 Sargassum bloom was massive enough that it became an issue of concern for both the Quintana Roo and national governments, particularly because of its potential adverse impact on tourism (Espinosa & Li Ng, 2020). An inter-ministerial commission coordinated by the Mexican Ministry of Tourism and Ministry of the Environment led aerial monitoring and cleaning efforts along more than 180 kms of coastline in Quintana Roo that year (Government of Mexico, 2015).

Figure 1. Volume of Sargassum (in tons), Quintana Roo

Year	Tons collected
2015	1,400
2016	1,500
2017	1,000
2018	522,226
2019	85,495
2020	19,054
2021	44,943
2022	29,243

Source: Rodríguez Martínez et al. (2016), Government of Quintana Roo (2019), Personal correspondence with the Ministry of the Environment of Quintana Roo, and reporting from Ángeles and Sánchez (2017).

Figure 2. Public interest in Sargassum, by region, measured by web search of the term

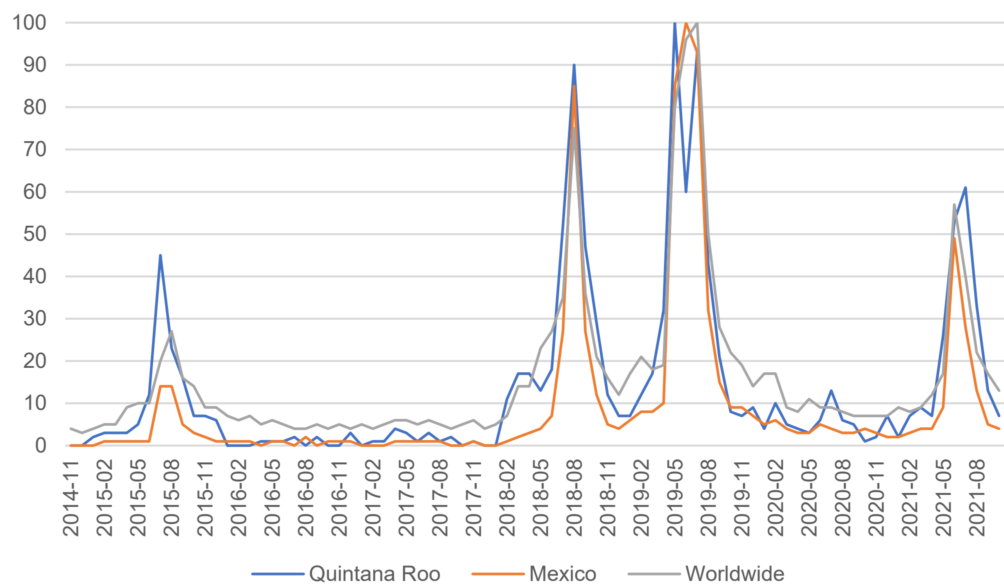

Note: The numbers represent the search interest relative to the highest point on the chart for the selected region and time. A value of 100 is the peak popularity of the term “sargazo” for Quintana Roo and Mexico and “Sargassum” for searches worldwide, whilst a value of 50 means that the term is half as popular.

Source: Google Trends (2021).

In the summer of 2018, Quintana Roo experienced extraordinary accumulations of Sargassum, and it remains as of today the year with the largest influx of the algae on record (see **Figure 1**). Public interest in Sargassum reached its peak among Quintana Roo citizens and Mexicans overall in the summer seasons of 2018 and 2019 (see **Figure 2**). Similarly, 2018 was also the first year on record with year-round occurrence of Sargassum blooms in the Caribbean Sea (Burrowes et al., 2019). During the period January-September 2022, approximately 29,000 tons of Sargassum were collected from the Quintana Roo shoreline.

The rest of the paper is organized as follows. Section 2 describes the multiple data sources we use to construct our outcome measures and covariates. Section 3 provides the empirical strategy that we use to answer two research questions: (i) does Sargassum posit an adverse effect on economic activity in coastal zones, and (ii) is this effect immediate or does it rather develop and persist over time? The answers to these questions are by no means obvious even if there is anecdotal evidence that Sargassum accumulation is linked to a decline in tourism. We propose a fixed-effects panel regression approach to estimate the impact of Sargassum on proxy indicators of economic activity. As we discuss in detail in this section, the premise of such a model is that we can control for omitted variable bias due to unobserved heterogeneity that is constant over time. Section 4 presents our main results as well as several robustness checks. Section 5 offers concluding remarks.

2 Data Description

2.1 General dataset design

Since the estimation of the impact of Sargassum on economic activity at the beach level is crucially linked to the location of the beaches in question, a logical design of the evaluation method is to structure data in a geographic information system (GIS). This structure allows the combination of spatial information for relevant beach characteristics with other types of information, including nighttime light intensity data. GIS has proven to be a useful tool to conduct economic analysis of spatially based problems by incorporating contextual features into the evaluation design, thus enabling researchers to combine relevant characteristics based on systematic data observations into a single map with multiple geographical layers. In a comprehensive review, Avtar et al. (2020) describe the multiple uses GIS and remote sensing can have in the context of measuring progress towards the United Nations' Sustainable Development Goals, highlighting that the scientific advances made in developing different spatial, spectral, radiometric, and temporal resolutions of geospatial data allow for an ever-increasing usage of such data in research and policy making.

In this context, a key condition of the spatial analysis is identifying the unit of observation of the GIS dataset. Geographically, the study area is restricted to the tourism-heavy coast of Quintana Roo state, in the Yucatán Peninsula of Mexico, which represents an approximate 1,000 km of shoreline between Holbox Island in the Northeast and Chetumal in the South. Since this study focuses on the impact of Sargassum in coastal areas and specifically on beach tourism, a logical choice for the unit of observation is the individual beach within the study area. Figure 3 depicts our study area: Quintana Roo State is highlighted in red within the Mexican territory in the upper lefthand corner of the map. The municipalities in which it is divided, and its shoreline, are represented by a red line in the larger map to the right of the figure. As we are only interested in the shoreline, our study focuses exclusively on the coastal municipalities displayed by name in the map.

Figure 3: Map of Quintana Roo and its coastal municipalities

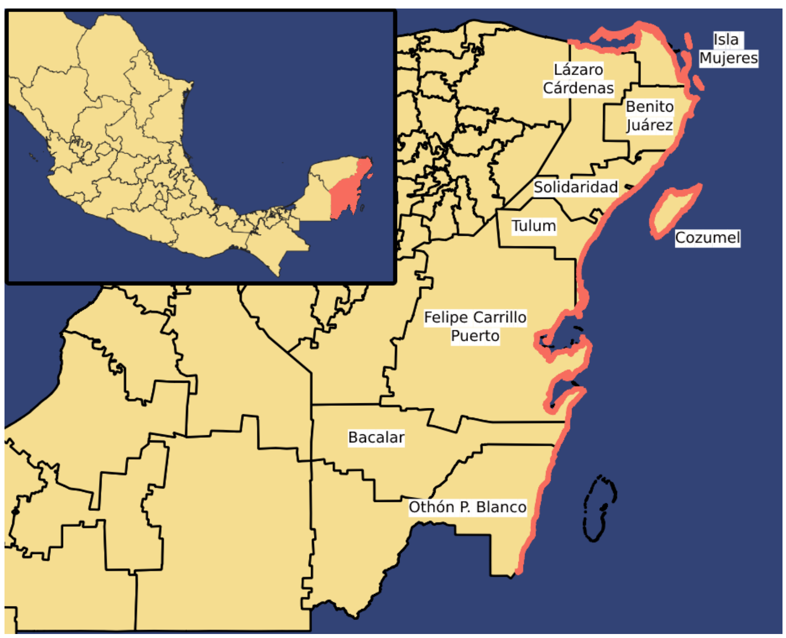

Since there are no established administrative boundaries separating the shoreline into individual beach units, the analysis relies on the division of beaches into so-called “segments” by applying the methodology developed by Cruz et al. (2019) for coastal geomorphic segmentation. In order to assess coastal anthropization based on local environmental, morphological and demographic variables, the authors identified shoreline segments according to the predominant type of coastal material, including sand, gravel, cliff, rocky, muddy and artificial infrastructure. Boundaries between segments were then established by identifying rivers, lagoon inlets, coastal structures or abrupt changes in coastline alignment. For the analysis, we removed any shoreline segments within large and small embayments because Sargassum detection in these ecosystems was not reliable. We also removed segments that delineated small, uninhabited islands. According to the geomorphological characterization and other criteria, our study area contains 157 shoreline segments, with an average length of 4.2 km and a total length of 656 km. Figure 4 presents two examples of shoreline segmentation according to Cruz et al. (2019) within our study area.

Figure 4. Examples of shoreline segmentation in study area

As depicted in Table 1, 60% of the identified shoreline segments consist of sand, which is in line with the touristic nature of Quintana Roo's sandy beaches. Approximately 30% of segments are made of cliff or rocky material, while only a small portion (5%) consist of artificial infrastructure.

Table 1. Descriptive statistics of shoreline segments

Geomorphic type	**Number of shoreline segments**
Artificial infrastructure	9
Cliff or rocky	49
Sand	99
Total	157

Figure 5. GIS dataset design

Dataset Layer	Variables Needed	Observational Unit	Type of Data	Data Source	Time Period / Frequency
Economic growth	Nighttime lights intensity (mean radiance)	450m pixel	Impact Indicator	VIIRS Day Night Band (DNB)	Oct. 2016 - Dec. 2019 (monthly)
Sargassum	Sargassum occurrence	Shoreline segment	Independent Variable	SENTINEL-2 Top of Atmosphere (TOA) imagery	Oct. 2016 - Dec. 2019 (monthly, with gaps)
Tourism activity	Number and distance of hotels, food & beverage, recreation & entertainment, archeological sites	Point location	Covariates	DENUE Reguero et al. (2019)	One-time observation
Coastal exposure	Shoreline length, geophysical type, wave energy, coastal vulnerability	Shoreline segment	Covariates	Natural Capital Project	One-time
Demographics and infrastructure	Population density Distance to key infrastructure	Population: 500m pixel Infrastructure: point or line location	Covariates	World Pop, Google Earth Engine	Annual (2016-2019), one-time

Note: Dataset layers are organized by the category of required data (impact indicator or category of control variables). The observational unit varies with the type of impact indicator (specifically for the nighttime lights intensity data), but the data is all aggregated to the individual beach segment.

Following this spatial division of the study area into beach segments, a comprehensive data collection effort was undertaken to identify and quantify various key attributes, such as beach exposure and characteristics of the surrounding infrastructure and demography. This was done with the objective of ensuring that a valid counterfactual for beaches with Sargassum can be identified, and that impact is estimated with attribution. Following the approach first proposed by Corral and Schling (2017), **Figure 5** above presents the design of the GIS dataset, which consists of five geographical layers that contain the relevant information for the purpose of this spatial and temporal analysis.

Because shoreline segment length is highly variable, ranging from 0.2 km to 40 km long, we calculated most of the spatial metrics using a set of regularly spaced points, 50 m apart, along the shoreline. These regularly spaced alongshore points were used to calculate metrics, like distances to infrastructure, and then values for the points were summarized by segment using an appropriate aggregation calculation, such as mean or minimum, depending on the metric.

2.2 Sargassum

Our main variable of interest is the detection of Sargassum along the Quintana Roo coastline, where its presence and accumulation on beaches may adversely affect tourism and overall economic activity. Satellite-based detection and monitoring of Sargassum has been successfully conducted for at least a decade. Many studies have applied straight-forward remote sensing indices, such as the Floating Algae Index (FAI) (Hu, 2009), the Maximum Chlorophyll Index (MCAI) (Gower et al., 2006), and the Alternative Floating Algae Index (AFAI) (Wang & Hu, 2016; Wang et al., 2019), which take advantage of the higher reflectance of the plants in the near-infrared region of the spectrum relative to surrounding features, such as water or bare beach substrate. Data using these methods to detect and monitor oceanic Sargassum distribution, density, and coverage are publicly available. For example, the University of South Florida's Sargassum Watch System (SaWS) produces Sargassum maps across the Caribbean Sea (and other regions around the globe) using the Floating Algae Index derived from MODIS, the Moderate Resolution Imaging Spectroradiometer satellite (NOAA, 2019), VIIRS, and Landsat 8 OLI satellite imagery.

Table 2. Count of unique Sentinel-2 image dates meeting maximum cloudy pixel percentage threshold by year

Year	Unique S-2 Image Date Counts
2015	2
2016	6
2017	18
2018	40
2019	41
All Years Combined	107

Despite significant advances in the remote detection and monitoring of floating Sargassum[1], most of these studies and efforts are focused on near real-time monitoring and forecasting of Sargassum in open waters and use coarse scale imagery (500-1000 m for MODIS), albeit with frequent revisit times (~1 day). For the purposes of this study, which focuses on historic trends of Sargassum, and not in the context of open water but along a geomorphologically diverse coastline, it is necessary to rely on higher resolution imagery to map historic Sargassum events on beaches and nearshore for individual shoreline segments. Therefore, a novel data processing approach was taken to generate a comprehensive dataset of historic Sargassum observations at medium frequency and higher spatial resolution.

Table 3. Count of unique Sentinel-2 image dates meeting maximum cloud pixel percentage threshold by month across all years

Month	Unique S-2 Image Date Counts
1 – January	3
2 – February	12
3 – March	11
4 – April	10
5 – May	10
6 – June	8
7 – July	9
8 – August	8
9 – September	9
10 – October	7
11 – November	9
12 – December	11

[1] See Hu et al. (2015) for a comprehensive review of measurement approaches that have been developed using various sensors with different spectral and spatial requirements.

We developed a remotely sensed time series of Sargassum distribution along beaches in Quintana Roo using satellite imagery from Sentinel-2 MSI for late 2016 through 2019. Sentinel-2 MSI imagery has a 10-meter pixel size in the visible spectral bands which allows reasonable spatial discrimination of the medium and larger nearshore accumulations of Sargassum that occur in Quintana Roo. Sentinel-2 has a 5-day revisit time, but due to cloudiness in the region, the availability of acceptable imagery is less frequent and on an irregular time step.

We accessed Level 1C Sentinel-2 imagery from Google Earth Engine (GEE) (Gorelick et al., 2017). Because of the dynamic nature of Sargassum occurrence along the shore, it is necessary to analyze imagery that covers the full study area per date in order to capture the spatiotemporal variability of the seaweed presence and coverage. Our study area is covered by six Sentinel-2 tiles (granules). For our analysis, we selected imagery only from dates that have less than 30% cloudy pixel percentage for at least five out of the six study region tiles. This criterion resulted in a range of time steps between image date and a variable number of images per year (Table 3).

Table 4. Optimized set of spectral bands and indices used for classification of nearshore Sargassum

Spectral Band	Description	Central wavelength	Pixel Size
B2	Blue band	493 nm	10 m
B5	Red edge band	704 nm	20 m
B8A	Near infrared (NIR) band	865 nm	20 m
B12	Shortwave infrared band	2190 nm	20 m
Index	**Description**		
FAI	Floating Algae Index		
SEI	Seaweed Enhancing Index		
NDVI	Normalized Difference Vegetation Index		
NDVI median	Annual median NDVI		
NDVI minimum	Annual minimum NDVI		
NDVI difference from median	Difference between single date NDVI and annual median NDVI		

Similar to Cuevas et al. (2018), we used a supervised random forest classification algorithm (Brieman, 2001) to classify image pixels into Sargassum versus several other land cover classes (other vegetation, clouds, unvegetated beach, and buildings). Prior to classification, the region to be classified was masked to exclude areas of the image that were definitely not Sargassum, including open water, terrestrial areas, and clouds. These preliminary masks are not perfect, especially the cloud masking, so some of these features remain in the pre-classified imagery, and therefore are included as land cover classes to train the random forest model. The non-Sargassum classes are grouped into the "Sargassum absent" class after the random forest classification.

Training and testing data for Sargassum and non-Sargassum classes were visually interpreted for a single date, (2019-05-07), guided by higher resolution imagery (PlanetScope) and presence/absence point locations from Sargassum Monitoring. A variety of spectral bands and indices were evaluated to optimize the inputs for the random forest model for nearshore Sargassum detection. The final set of bands and indices are shown in Table 4.

Figure 6 displays a visual representation of how Sargassum was detected and classified using the applied approach. Panel (a) shows a sample false color Sentinel-2 image for a date with minimal Sargassum (2021-12-03); Panel (b) shows the same region from a date with a large Sargassum influx (2021-05-07); and Panel (c) then shows the result of the image classification for the second date, with the detected Sargassum pixels highlighted in magenta. The comparison of two dates demonstrates the value of including a multitemporal input to the classification (i.e., NDVI difference) along with individual bands and indices from the date of interest. Because the Sargassum presence is dynamic, a comparison between time periods can highlight the areas with Sargassum.

Figure 6. Visual example of Sargassum detection and classification

Panel (a) *Panel (b)* *Panel (c)*

The output from the random forest classification was tested with additional validation points randomly selected from six image dates across all seasons and representing a range of low to high Sargassum abundance. The overall accuracy for Sargassum vs. non-Sargassum classification for all dates, as a percentage of correctly classified polygons, ranged from 74% to 99%. Table 6 shows that the accuracy is generally better for the higher abundance time periods, but the slightly lower accuracies in September, November and December are acceptable and may be an artifact of the lower number of Sargassum polygons available for validation.

For the final data, all pixels within 100 meters of the shoreline are classified into one of three classes: Sargassum present, Sargassum absent, and no data (cloudy pixels). The pixel count for each of the three classes is assigned to the adjacent shoreline segment by date. This final data set shows the spatial and temporal variability of Sargassum distribution along beaches in Quintana Roo for a period of four years, from October 2016 to December 2019.

For the purpose of this analysis, Sargassum presence at a beach segment is measured as a dummy variable that takes the value 1 if any Sargassum was detected in beach segment b in month t. As a fairly large amount of Sargassum is necessary for it to be detected through satellites, we consider the detectable level of Sargassum sufficient to have an impact on local economic activity.[2]

Table 5. Overall Sargassum presence/absence classification accuracy for seven image dates in 2019

Date	**Overall accuracy Sargassum presence / absence % polygons correct**
2019-02-26	93%
2019-04-02	90%
2019-05-07 *(training date)*	99%
2019-06-26	92%
2019-09-14	81%
2019-11-18	83%
2019-12-03	74%
All dates Combined	88%

[2] It should be noted that beach segments for which Sargassum presence was detected in every observed time period are automatically excluded from the analysis (see Section 3) since lack of variation prevents the estimation of an effect for such locations. This accounts for a total of 7 beach segments (4% of sample).

Figure 7 shows the percentage of beach segments in the sample where the presence of Sargassum was detected per quarter, as defined in the previous paragraph. It can be observed that this indicator follows a similar trend as that reported in Figure 2. Following this trend, it is interesting to note that during the first semester of 2018 and the first quarter of 2019, Sargassum was detected in more than 80% of beach segments in the sample.

Figure 7. Quarterly trend of Sargassum presence

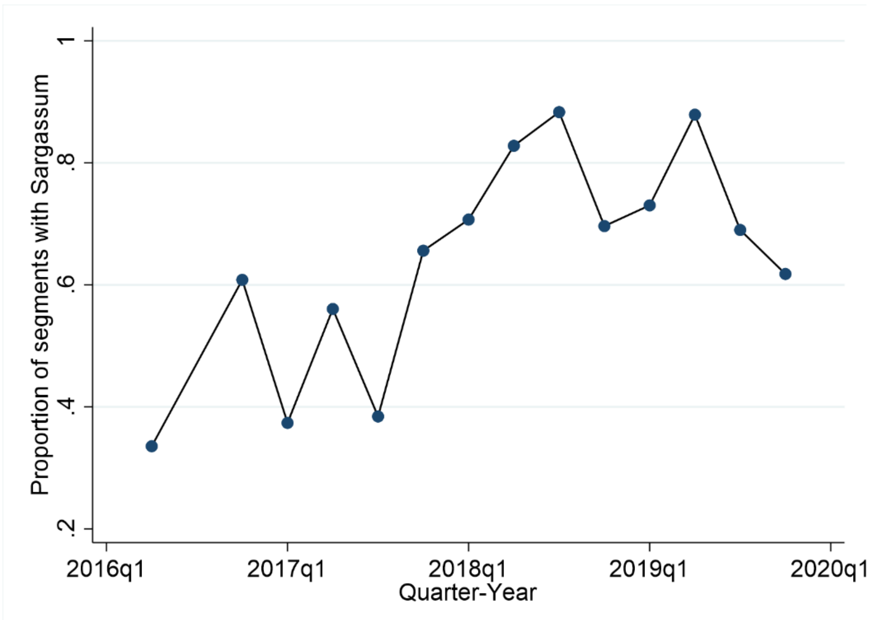

2.3 Nighttime light intensity as a proxy of economic activity

The principal impact that we assess is the effect of the presence of Sargassum on economic activity at the shoreline segment level. For the state of Quintana Roo, the National Institute of Statistics and Geography of Mexico (INEGI) provides variables that are traditionally used to measure economic activity, such as gross domestic product (GDP), the employment or the investment rate, only at the state, or, at best, the municipal level, which is too large a spatial aggregation to capture changes in economic activity as a result of Sargassum impacts. Given the unavailability of traditional measures of economic activity at sufficiently small beach segments necessary for the purpose of this impact evaluation, we rely on remotely sensed nighttime light intensity data to approximate economic activity.

Nighttime light intensity, or luminosity, has been recorded by satellite sensors since the 1970s. Between 1992 and 2013, the United States Air Force Defense Meteorological Satellite Program (DMSP) used so-called Operational Linescan System (OLS) sensors to detect Earth-based lights (Henderson et al., 2012). In 2012, the Visible Infrared Imaging Radiometer Suite (VIIRS) sensor of the Suomi National Polar-Orbiting Partnership (NPP) satellite started recording global observations on light intensity and replaced DMSP-OLS. Among 22 spectral bands, the NPP-VIIRS provides the Day/Night Band (DNB) that allows the measurement of nighttime lights intensity with a 15 arc second spatial resolution, which translates to a latitude-longitude grid of rectangular pixels of approximately 500 m^2 size (Ivan et al., 2020). Using this imagery, the Earth Observations Group (EOG) at the National Oceanic and Atmospheric Administration (NOAA)'s National Centers for Environmental Information (NCEI) makes monthly cloud-free average radiance composites available for public use (EOG, 2021).[3] We use Google Earth Engine (GEE) to obtain the monthly average radiance composite generated by EOG (GEE, 2021). For each grid pixel, nighttime light intensity is measured in nanowatts per square centimeter per steradian, or $nW/(cm^2 \cdot sr)$[4] (Cao & Bai, 2014). It should be noted that in comparison to the earlier DMSP-OLS sensors, the newer NPP-VIIRS data have the advantage of providing higher resolution imagery (compared to the 13 arc second spatial resolution of DMSP-OLS) and higher frequency (with daily images available instead of only monthly composites), benefit from the satellites' on-board calibration capabilities that allow consistency in measurements over time, have a higher sensitivity to lower light levels, and do not suffer from oversaturation in bright regions, allowing for a more precise estimation of socio-economic activity (Jing et al., 2016; Levin et al., 2020).

Numerous studies (e.g. Elvidge et al., 1997; Sutton and Costanza, 2002; Ghosh et al., 2010; Henderson et al., 2012; Kyba et al., 2017) have established that there exists a positive, linear relationship between a positive economic growth and greater lights usage per person. A key advantage over most socio-economic indicators which typically rely on census data or similar administrative data, is that light emission can be measured instantaneously, objectively, and systematically at considerably high resolution (Cauwels et al., 2014; Levin et al., 2020). Considering the dearth of reliable socioeconomic data, particularly in the developing world, multiple studies have relied on nighttime light intensity data as a proxy for economic growth to carry out empirical analysis at low levels of spatial disaggregation. In a study focusing on intra-city economic development, Agnew et al. (2008) assess the effect of the U.S. military surge into specific neighborhoods of Baghdad in 2007 on levels of violence and consequently the quality of life. Storeygard (2013) uses nighttime light intensity to investigate the effect of inter-city transport costs on urban economic activity in sub-Saharan Africa. Alesina et al. (2016) employ nighttime light intensity data combined with the historical location of ethnolinguistic groups to construct an

[3] Elvidge et al. (2017) provide a detailed description of how nighttime lights metric is constructed from VIIRS imagery.
[4] The radiance dynamic range lies between 5×10^{-11} $W/cm^2 \cdot sr^1$ to 0.02 $W/cm^2 \cdot sr$.

index of ethnic income inequality in over 150 countries. In a recent study, Corral and Schling (2017) employ nighttime light intensity to evaluate the local economic impact of a shoreline stabilization program in Barbados, while another study by Corral et al. (2018) relies on nighttime light intensity to estimate the economic impact of Peru's largest hydrocarbon project at the department level.

Figure 8. Nighttime light intensity as a measure of economic activity

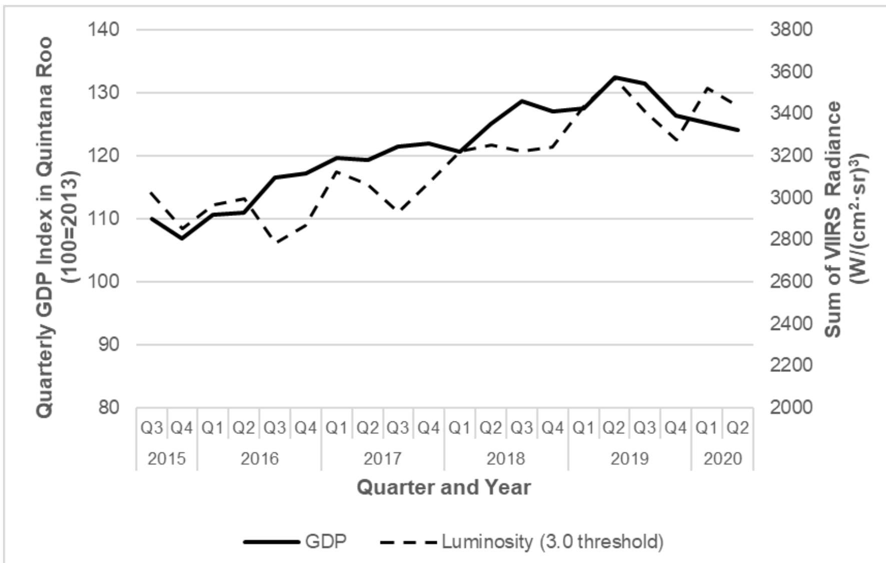

(i) GDP and nighttime light intensity over time

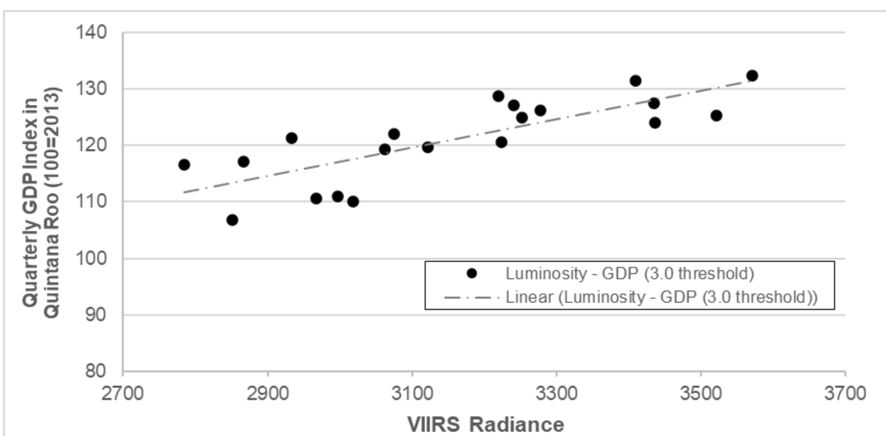

(ii) Plotting GDP vs. nighttime light intensity

While we cannot directly assess the relationship between nighttime light intensity and economic activity at the beach segment level, we examine how closely the two measures correlate at the smallest possible level of geographic resolution. In our case, this happens to be at the State level, since INEGI provides quarterly data on gross domestic product (GDP) for Quintana Roo and all other Mexican states.[5] Figure 8 presents a visualization of this relationship.

Figure 9. Quarterly trend of nighttime light intensity

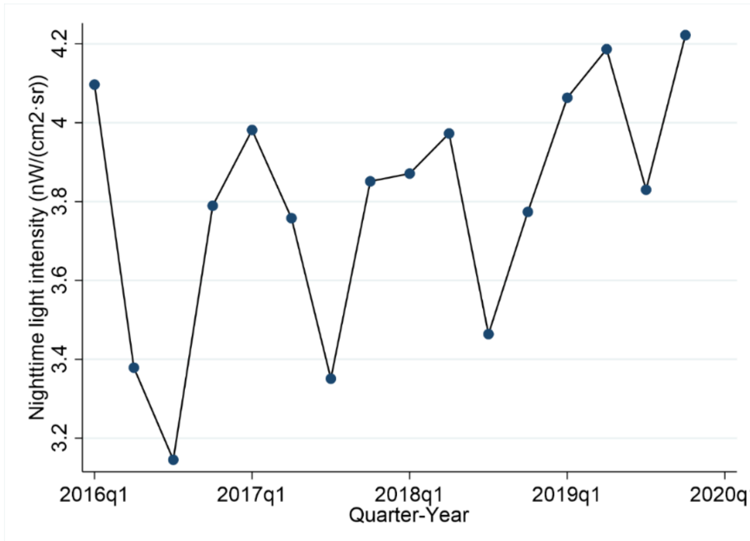

In Panel (i), we observe the trend of VIIRs radiance and state-level GDP over time, for the study period of the second half of 2015 until the second quarter of 2020. As can be seen, there is a gradual increase in both economic growth and VIIRs radiance for the state as a whole, suggesting that a parallel trend holds for both measures. Panel (ii) illustrates this close relationship by plotting GDP against nighttime light intensity, indicating that a clear linear and positive relationship holds for the two measures. Quantitatively, this relationship can be confirmed by estimating the Pearson's correlation coefficient, with a robust value of 0.839. Similarly, the R^2 for the linear regression exhibits a value of 0.703, further confirming that nighttime light intensity can account for a significant share of variance observed in quarterly economic activity. Lastly, in order to determine quantitatively how a change in nighttime light intensity translates to a change in GDP, the elasticity is also of interest. Studies carried out by Elvidge et al. (1997), Henderson et al. (2012) and others have found that, depending on country context, elasticity of GDP to nighttime light intensity tends to lie in the magnitude of 1. As presented in Appendix A, in the case of Quintana Roo a simple log-log regression indicates an elasticity of 0.66. Of course, when interpreting the results of this study, it will be important to note that the relationship between gross

[5] Because the VIIRS Day Night Band (DNB) has higher sensitivity to lower light levels, it is subject to detection of dim light sources that are not anthropogenic (Coesfeld et al. 2020) or scattered from other areas (Miguel et. al. 2020). The effect of this sensitivity is exacerbated when calculating the sum of lights across large areas with minimal or no anthropogenic lighting, such as Quintana Roo. Therefore, a common approach is to set a minimum radiance threshold for calculating further metrics from the radiance pixels in order to avoid having many small, but potentially spurious values obscure important patterns of economic activity. For our correlation analysis with GDP, we set the minimum radiance threshold at 3.0 nW/cm^2/sr.

local product and nighttime light intensity may differ at the beach level, so that the exact estimation of changes in nighttime light intensity will present an approximation of changes in gross local product at this level.

To summarize, the final dataset for nighttime light intensity that will be used to carry out the analysis consists of monthly observations for the period between October 2016 and December 2019, for 157 shoreline segments along the coast of Quintana Roo State in Mexico. Figure 9 presents quarterly average for nighttime light intensity at the beach segment level. As expected, nighttime light intensity exhibits certain seasonality in accordance with the highs and lows of tourism activity, which peaks during winter and early spring in Quintana Roo and is generally lower during the hot summer months.

2.4 Additional Covariates

In addition to the main variables of interest, we obtained a number of variables to characterize each shoreline segment as presented in Figure 5. The first group of these characteristics consists of basic infrastructure and demographic information about the study area, including the location of and distance from the beach segment to key infrastructural sites such as major roads, airports and ports. The infrastructure data were compiled from a variety of freely available sources (including Natural Earth, Humanitarian Data Exchange, and MapCruzin.com) and supplemented by information from local experts. In order to link this data to the individual beach segment, we measured the distances to these features from each 50m alongshore point and calculated the minimum and mean distance by segment. Additionally, we include annual population density obtained from WorldPop, which bases its estimates on available census information to project annual changes in population and uses geospatial datasets to disaggregate them to counts for 100m x 100m grid (WorldPop, 2020). In order to accommodate differences between the shoreline location and the WorldPop raster, we aggregated the 100m pixels by summing them into 500m pixels. Then, we sum all population counts across each shoreline segment for the years 2016-19.

The next group compiles information on the beach geomorphology, wave exposure and coastal vulnerability of the shoreline segments, a crucial determinant in the context of this study given the relevance of beach tourism in the study area and the potential impact that the presence of Sargassum may have on it. Beach attributes include the total length of the shoreline segment and the geophysical beach type (sand, rock, mud, artificial) (Cruz et al. 2019). Furthermore, additional metrics developed by the Natural Capital Project at Stanford University provide a measure of wave dynamics that may affect both the inflow of Sargassum and how attractive the shoreline is from a recreational perspective. These metrics include relative wave exposure, and the coastal exposure index derived from the InVEST Coastal Vulnerability (CV) model (Sharp et al. 2020) which has been applied around the world to assess risk from coastal hazards (Arkema et al. 2013, Cabral et al. 2017, Silver et al. 2019). Relative wave exposure is calculated from historical wind speed, wave height, and wave power; fetch distance (distance to nearest point of land); and mean bottom depth in sixteen cardinal directions. A given stretch of shoreline is generally exposed to either oceanic waves or locally generated, wind-driven waves. The coastal exposure index synthesizes multiple ranked biophysical variables, including geomorphology, relief, natural habitats, wave exposure, wind exposure, and surge potential, into a single value calculated as the geometric mean of all variable ranks. The ranks range from 1 (very low exposure) to 5 (very high exposure).[6]

The last set of covariates characterizes the extent of touristic activities taking place near each beach segment. For this purpose, we include information on the number of hotels (with a separate measure for the number of five-star hotels) and other lodging facilities, as well as the number of food and beverage facilities located within 1 km from the shoreline. This information was extracted from the Mexican Institute of Statistics' National Statistical Directory of Economic Units (DENUE), which provides infrastructure data for the period 2010-2020 (INEGI, 2020). Information on five-star hotels was obtained from a study by Reguero et al. (2019). We also include the mean and minimum distances to the nearest lodging or food and beverage establishment from each beach segment aggregated from the 50m regularly spaced alongshore points. Furthermore, we include the count within 1 km and distance to nearest recreation and entertainment businesses, and archeological sites from the beach segment. The latter is included given their prevalence and touristic appeal along the Quintana Roo coast. Based on the hypothesis that the availability of lodging and recreational activities affects overall economic and touristic activity at the local level, these covariates will be relevant to control for other factors determining local economic activity at each beach segment.

Table 6 presents the segment-level variables included in our data. To present the variety of beach segments in our sample, we group beach segments according to municipality, as the second-level administrative division in Mexico, below the state level. According to municipality-level divisions along the Quintana Roo shoreline, we sorted beach segments according to their location in the municipalities with heavy concentration of touristic activities, namely Benito Juárez (including Cancún), Solidaridad (including Playa del Carmen), Tulum, and Cozumel. The remaining beach segments were assigned either to the category of "small islands", which included

[6] See the user guide for the InVEST CV model (Sharp et al., 2020) for more details on how coastal vulnerability indicators are measured.

Table 6. Summary statistics by municipality

	Benito Juárez (Cancún)	Solidaridad (Playa del Carmen)	Tulum	Cozumel	Small Islands	Rest of Mainland	Total
Number of beach segments	17	50	24	33	13	20	157
Basic infrastructure and demographic information							
Population density (2018)	3.48 (4.13)	1.29 (2.55)	1.01 (1.24)	1.47 (4.11)	3.46 (9.01)	0.55 (1.99)	1.55 (4.16)
Mean distance to nearest road (km)	0.96 (0.96)	1.17 (0.47)	0.76 (0.74)	4.99 (5.30)	17.46 (11.65)	15.62 (14.46)	6.96 (10.80)
Mean distance to nearest airport (km)	13.29 (5.72)	28.40 (6.27)	56.38 (17.50)	13.46 (7.22)	16.38 (13.34)	47.94 (43.12)	31.23 (27.88)
Mean distance to nearest port (km)	5.58 (5.76)	10.40 (5.68)	10.43 (5.36)	14.19 (7.51)	16.04 (12.68)	20.74 (17.55)	13.68 (11.74)
Beach geomorphology, wave exposure and coastal vulnerability							
Segment length (km)	3.49 (4.25)	1.40 (1.49)	6.47 (10.75)	3.84 (4.73)	8.86 (8.89)	14.67 (20.90)	6.62 (12.55)
Coastal vulnerability index: Exposure	2.77 (0.34)	2.07 (0.31)	2.45 (0.31)	1.97 (0.42)	2.89 (0.62)	2.70 (0.32)	2.33 (0.50)
Costal vulnerability index: Wave intensity	22.05 (9.17)	7.09 (7.16)	21.35 (7.94)	17.24 (14.85)	20.47 (14.83)	31.75 (6.16)	17.32 (13.03)
Touristic activities							
Count of hotels within 1km	12.22 (18.59)	16.42 (45.66)	5.14 (6.89)	3.80 (9.61)	8.77 (15.34)	1.09 (3.27)	7.91 (25.60)
Count of 5-star hotels within 1km	0.61 (0.95)	0.16 (0.88)	0.00 (0.00)	0.00 (0.00)	0.00 (0.00)	0.15 (0.63)	0.13 (0.64)
Count of lodging within 1km	12.44 (16.67)	12.16 (39.46)	7.79 (14.52)	4.59 (12.21)	19.27 (30.13)	1.48 (5.26)	8.56 (24.87)
Count of food & beverage within 1km	25.28 (29.00)	31.36 (98.48)	5.34 (8.58)	28.34 (85.91)	42.61 (77.55)	2.14 (9.86)	21.29 (69.09)
Count of entertainment & recreation within 1km	4.61 (6.11)	3.82 (9.00)	1.65 (1.98)	5.21 (14.33)	2.67 (6.17)	0.37 (1.77)	2.92 (8.31)
Mean distance to nearest lodging (km)	0.49 (0.46)	1.29 (1.19)	1.44 (1.50)	6.61 (5.97)	13.32 (12.09)	14.67 (11.59)	6.64 (9.44)
Mean distance to nearest food & beverage (km)	1.08 (1.11)	2.61 (2.36)	2.70 (3.65)	2.88 (3.58)	9.60 (10.07)	19.08 (17.05)	7.17 (11.57)
Mean distance to nearest entertainmt. & rec. (km)	1.41 (1.30)	1.37 (1.20)	5.99 (10.05)	5.16 (3.86)	15.20 (13.41)	28.37 (20.48)	10.51 (15.78)
Mean distance to nearest archaeological site (km)	10.39 (10.36)	10.82 (6.10)	10.24 (8.27)	9.38 (4.09)	41.48 (22.12)	52.35 (21.94)	23.60 (23.34)

all islands except for Cozumel, and "rest of mainland" for those beach segments located outside the municipalities named above.

To link beach segments to municipalities, we used geospatial data on Mexican subnational administrative boundaries obtained from the INEGI. It should be noted that these municipality-level groupings vary in number of segments, as well as in their characteristics. For example, beach segments assigned to the "rest of mainland" category are considerably longer than those in Solidaridad. However, beach segments in Solidaridad have on average almost 16 times more hotels within a 1 km radius than those in the rest of the mainland. Another striking difference comes in terms of population density in 2018, as beach segments like those in Benito Juárez are very densely populated, while those in the rest of the mainland are not. This, of course, will have an impact on the perceived nighttime light intensity, and therefore it is important to control for it.

3 Empirical Approach

3.1 Basic model

Since we expect the presence of Sargassum to vary over time and in a manner that is not uniform across all beach segments, we propose to use a fixed-effects panel regression approach to estimate the impact of Sargassum on nighttime light intensity. It is worth mentioning that, as reviewed in Section 1, the presence of Sargassum has a cyclical component in the Quintana Roo area. However, the influx of Sargassum at a specific beach and at a certain moment in time, should be unrelated to economic activity or nighttime light intensity, since it depends entirely on geomorphological characteristics of the segment as well as offshore wave dynamics that are not correlated with local economic activity. Therefore, for a given beach segment in a given time period, exposure to Sargassum should be considered exogenous.

The proposed fixed effect method permits controlling for time-invariant, unobserved heterogeneity across beach segments (Stock and Watson, 2011). The regression should therefore take the following form:

$$y_{bmt} = \alpha Sarg_{bt} + \boldsymbol{x}'_{bt}\boldsymbol{\beta} + \gamma_t + \delta_m + \varepsilon_{bt} \qquad (1)$$

where $\boldsymbol{y_{bt}}$ represents nighttime light intensity in beach in month t and beach segment b located in municipality m, $\boldsymbol{Sarg_{bt}}$ represents a dummy variable that takes on the value 1 if Sargassum is detected in beach segment b during month t, and $\boldsymbol{x'_{bt}}$ is a vector of beach segment-level covariates. The segment-level controls include the following covariates that were described in Section 2: beach length, coastal vulnerability, wave intensity, population density, number of hotels within a 1 km radius and number of 5 stars hotel within a 1 km radius, as well as the distance in kilometers to the nearest archeological site, port, airport, road, entertainment center and lodging. Parameter $\boldsymbol{\gamma_t}$ reflects monthly time fixed effects and parameter $\boldsymbol{\delta_m}$ reflects municipality-level fixed effects. Vector $\boldsymbol{\beta}$ and coefficient $\boldsymbol{\alpha}$ are the parameters to be estimated. $\boldsymbol{\varepsilon_{bt}}$ is the error term.

Coefficient α should then be a bias-free estimate of the effect of Sargassum presence on nighttime light intensity at the beach segment level. It should be noted that for panel data, it is possible that regression errors are correlated over time within an entity, which would, similarly to heteroscedasticity, affect the estimation of standard errors. In order to account for the potential of autocorrelation among regression errors, we employ municipality-level clustered standard errors, which allow for heteroskedasticity and autocorrelation within an entity (in our case, the municipality), but not across entities (Moulton, 1986).

3.2 Reputation effects

Our hypothesis posits that Sargassum has an adverse effect on economic activity in beach segments where it washes ashore. However, it is possible that this negative effect is not immediate but rather develops over time as the reputation of the attractiveness of a beach segment is affected negatively by Sargassum. For instance, tourists may not react to the presence of Sargassum by immediately leaving the beach: Even if Sargassum accumulation on the shoreline may affect their enjoyment of the beach, because they may not be able to swim in the ocean, or are bothered by the smell of the drying algae, it may be difficult for tourists to leave their vacation spot once they are already there, since they would face cancellation and other opportunity costs for departing early from their vacation. Even if tourists have not yet arrived in the area, it may be difficult for them to change their holiday plans on short notice, especially if plane tickets or hotel rooms have already been booked. It also unlikely that tourists may hear about the presence of Sargassum in advance within a few weeks prior to arrival. Thus, impacts of Sargassum presence on local economic activity may not be as sizeable in the immediate time period following the influx.

A negative reputation effect is therefore more likely to occur several months after Sargassum was washed ashore on a beach. This may be because news may circulate about significant Sargassum presence in the area (see Figure 2), disincentivizing tourists that are still deciding on a vacation spot, or because tourists had a negative experience with Sargassum on their last trip and are unlikely to return to the same spot in the following holiday season. To capture this possible reputation effect, we propose a model that incorporates time lags on the effects of Sargassum, as described by the following model:

$$y_{bmt} = \sum_{i=0}^{T} \alpha_i Sarg_{bt-i} + \boldsymbol{x}'_{bt}\boldsymbol{\beta} + \gamma_t + \delta_m + \varepsilon_{bt} \qquad (2)$$

In this specification, we include multiple time lags, $i = 0, \dots, T$, for Sargassum presence at a beach segment b, ranging from 0 to 12 months. As a result, the updated model includes $T + 1$ number of $\boldsymbol{\alpha_i}$ parameters ($\boldsymbol{\alpha_0}, \boldsymbol{\alpha_1}, \boldsymbol{\alpha_2}, \dots, \boldsymbol{\alpha_T},$) to be estimated, where $\boldsymbol{\alpha_i}$ measures the effect of Sargassum presence on nighttime light intensity in beach segment b in month t, i months after Sargassum was detected. All other variables remain the same as in specification (1).

3.3 Spatial correlation

Another potential dynamic at play in the relationship between Sargassum and nighttime light intensity concerns potential spatial correlation. To understand how this could occur, we must first consider that the nature of our data is quite unique, as beach segments are defined as line segments of a continuous line that follows the Quintana Roo shoreline.[7] Thus, we can conceptualize space in our data as linear. As beach segments are contiguous, the linear nature of the data implies that each beach segment has a maximum of two neighboring beach segments.[8] If we were to put beach segments on a line, we could number these beach segments $b = 1, \dots, B$. To formalize this concept, we will refer to the neighbors of beach segment b as beach segments $b - 1$ and $b + 1$.

Spatial correlation in our analysis might come through different channels. The first, and perhaps most important, is that nighttime light intensity in beach segments b might be influenced by nighttime light intensity in its neighboring beach segments. As explained in Section 2, nighttime light intensity was assigned to beach segments by proximity, making it possible that some light radiance pixels assigned to construct the nighttime light intensity for beach segment $b + 1$ might have also been used to construct nighttime light intensity for beach segment b.

Secondly, spatial correlation between neighboring beach segments may occur through the effects of Sargassum. As Sargassum washes ashore beach segment b, it is possible for tourists to crowd out from the area and move to a neighboring beach segment that is less affected by the algae. Alternatively, if Sargassum washes ashore one beach segment, it may also be more likely to be present in the neighboring segments if wave currents and geomorphology favor the arrival of the seaweed along the extended shoreline. Either way, through this channel local economic activity in neighboring beach segments $b - 1$ and/or $b + 1$ may be affected when Sargassum washes ashore segment b.

[7] The only exception to this definition concerns some islands (the island of Cozumel being the largest), for which beach segments are still individual line segments as part of a larger continuous shoreline, with the exception that they do not form part of the mainland's shoreline.

[8] Some beach segments at the edge of the Quintana Roo territory or on small islands might only have 1 neighbor.

Assuming spatial correlation between immediate beach segments only, we implement the following spatial autoregressive (SAR) model with time lags:

$$y_{bt} = \sum_{i=0}^{T} \alpha_i Sarg_{bt-i} + \sum_{i=0}^{T} \tau_{1,i} y_{b+1,t-i} + \sum_{i=0}^{T} \tau_{2,i} y_{b-1,t-i} + \sum_{i=0}^{T} \rho_{1,i} Sarg_{b+1,t-i} + \sum_{i=0}^{T} \rho_{2,i} Sarg_{b-1,t-i} + \boldsymbol{x}'_{bt}\boldsymbol{\beta} + \gamma_t + \delta_m + \varepsilon_{bt} \quad (3)$$

where $y_{b+1,t-i}$ and $y_{b-1,t-i}$ represent nighttime light intensity for month $t-i$ in neighboring beach segments $b+1$ and $b-1$, respectively; $Sarg_{b+1,t-i}$ and $Sarg_{b-1,t-i}$ are dummy variables that take the value of 1 if Sargassum is detected for month $t-i$ in beach segments $b+1$ and $b-1$. The parameters to be estimated are $\boldsymbol{\alpha}_{\boldsymbol{1},\boldsymbol{i}}, \boldsymbol{\beta}, \boldsymbol{\tau}_{\boldsymbol{1},\boldsymbol{i}}$, $\boldsymbol{\tau}_{\boldsymbol{2},\boldsymbol{i}}$, $\boldsymbol{\rho}_{\boldsymbol{1},\boldsymbol{i}}$, $\boldsymbol{\rho}_{\boldsymbol{2},\boldsymbol{i}}$; and $\boldsymbol{\varepsilon}_{\boldsymbol{bt}}$ is the error term. To examine the channel of spatial correlation through nighttime light intensity, we first assume that $\boldsymbol{\rho}_{\boldsymbol{1},i} = \boldsymbol{0}$, $\boldsymbol{\rho}_{\boldsymbol{2},i} = \boldsymbol{0}$, for a specification we will denominate SAR-1. Then, to allow for both channels of spatial correlation, we include all parameters in a specification we will refer to as SAR-2. All estimations included clustered standard errors at a municipality level.

It is important to note that there exist other potential channels of spatial correlation that our model does not take into consideration. For example, it is possible that a beach segment is not only affected by the immediate neighbor, but also by the neighbor(s) next to it. This could be the case for one, two or even more neighboring beach segments. It is also possible that neighboring beach segments are correlated not through the presence of Sargassum or nighttime light intensity, but through other observed and unobserved variables. However, we do not believe these are relevant concerns in this context, for two reasons. First, the basic specification of the model already accounts for municipality-level fixed effects that control for time-invariant characteristics across beach segments located within the same municipality. By doing so, we indirectly control for some potential spatial correlation that might arrive from geopolitical divisions. Second, because the presence of Sargassum at a given time and in a specific beach segment is considered exogenous, the estimation should be unbiased, regardless of other sources of spatial correlation within the model.

4 Results

4.1 Main Results

Table 7 presents the effects of Sargassum detection on nighttime light intensity at the beach segment level. Following equation (1), three different specifications were used in our estimations. First, we implement a basic model in which we only controlled for time-fixed effects (Column 1), which assumes no municipality fixed-effects and no segment-level controls. Second, to account for time-invariant differences between municipalities and to control for beach segment specific characteristics, we introduce municipality-level fixed effects and segment-level controls (Column 2). Third, we include municipality-level clustered standard errors (Column 3).

Table 7. Effects on nighttime light intensity with no lag

	Nighttime light intensity		
Variables	(1)	(2)	(3)
Sargassum detected in the same month (t=0)	**-1.852***** (0.213)	**-0.813***** (0.130)	**-0.813**** (0.241)
Time fixed effects	Yes	Yes	Yes
Segment-level controls		Yes	Yes
Municipality-level fixed effects		Yes	Yes
Municipality-level clustered standard errors			Yes
Number of observations	5,371	5,371	5,371
Adjusted R^2	0.261	0.745	0.745

Results show that having detectable Sargassum in a beach segment significantly reduces nighttime light intensity, by 1.85 nW/(cm^2·sr) for the simplest model, and by 0.81 nW/(cm^2·sr) when controlling for segment-level covariates and municipality-level fixed-effects. These results remain equally significant when adding municipality-level cluster standard errors. Considering an average level of 4.63 nW/(cm^2·sr) among beaches in the dataset, this implies an average reduction of 17.5% of local economic activity. Using the estimated elasticity of 0.66 between state-level nighttime light intensity and gross local product, this suggests an approximate decrease of monthly economic growth of 11.6% for the more rigorous specifications.

4.2 Reputation Effects

To account for reputation effects of Sargassum on economic activity, we include monthly time lags in our estimation. Results including a one-month lag are presented in Table 8. Once again, column 1 shows results when controlling for time fixed effects only, column 2 includes municipality-level fixed effects and segment-level controls, and column 3 adds municipality-level clustered standard errors. Results again show significant negative effects of Sargassum detected in all models. It is worth noting that effects after a month of exposure to the shock are larger than those at the month of nighttime light intensity measurement, for all models.

Table 8. Effects on nighttime light intensity with 1 month lag

	Nighttime light intensity		
Variables	(1)	(2)	(3)
Sargassum detected in the same month (t=0)	**-1.314*****	**-0.676*****	**-0.676****
	(0.244)	(0.142)	(0.216)
Sargassum detected 1 month prior (t=1)	**-1.432*****	**-0.680*****	**-0.680***
	(0.248)	(0.142)	(0.322)
Time fixed effects	Yes	Yes	Yes
Segment-level controls		Yes	Yes
Municipality-level fixed effects		Yes	Yes
Municipality-level clustered standard errors			Yes
Number of observations	4,800	4,800	4,800
Adjusted R^2	0.266	0.751	0.751

To test if reputational effects persist in the medium- and long term, we estimate the same model with a 3-, 6- and 12 month-lags, respectively. Table 9 reports these results for our most rigorous model, which includes time fixed-effects, municipality-level fixed effects, beach segment controls, and clustered standard errors. Results for an estimation only considering 3-months lags are reported in Columns 1. Columns 2 and 3 report results for estimations including a 6-months lag and a 12-months lag, respectively.

Results for the effect of Sargassum detection on nighttime light intensity continue to be negative and largely statistically significant for all models and lags; and vary between 0.42 and 0.73 nW/(cm^2·sr) in magnitude. This roughly translates into a 5.9-9.9% reduction in monthly economic activity using the elasticity approximation. Interestingly, the more lags we add, the smaller our effects for the initial periods get. For our last model that included a 12-month lag, our effects for month of Sargassum presence (t=0) appear insignificant and small, although still negative. Over time, these effects continue to grow larger and size and become statistically significant.

Table 9. Effects on nighttime light intensity with 3-, 6- and 12-month lags

	Nighttime light intensity		
Variables	(1)	(2)	(3)
Sargassum detected in the same month (t=0)	**-0.631***** (0.151)	**-0.444**** (0.134)	-0.030 (0.112)
Sargassum detected 1 month prior (t=1)	-0.549 (0.298)	**-0.484*** (0.248)	-0.191 (0.228)
Sargassum detected 2 months prior (t=2)	**-0.546*** (0.275)	-0.415 (0.220)	-0.279 (0.211)
Sargassum detected 3 months prior (t=3)	**-0.520**** (0.214)	-0.346 (0.183)	-0.257 (0.167)
Sargassum detected 4 months prior (t=4)		**-0.520**** (0.166)	**-0.420*** (0.182)
Sargassum detected 5 months prior (t=5)		**-0.588**** (0.188)	**-0.595**** (0.191)
Sargassum detected 6 months prior (t=6)		**-0.734***** (0.179)	**-0.626**** (0.218)
Sargassum detected 7 months prior (t=7)			**-0.403**** (0.137)
Sargassum detected 8 months prior (t=8)			**-0.456**** (0.144)
Sargassum detected 9 months prior (t=9)			**-0.684***** (0.185)
Sargassum detected 10 months prior (t=10)			-0.448 (0.243)
Sargassum detected 11 months prior (t=11)			**-0.624**** (0.240)
Sargassum detected 12 months prior (t=12)			**-0.670**** (0.283)
Time fixed effects	Yes	Yes	Yes
Segment-level controls	Yes	Yes	Yes
Municipality-level fixed effects	Yes	Yes	Yes
Municipality-level clustered standard errors	Yes	Yes	Yes
Number of observations	4,200	3,600	2,700
Adjusted R^2	0.755	0.761	0.770

In order to visually examine the dynamics of the reputation effects, Figures 10 and 11 present graphs with the results in columns 2 and 3 of Table 3. The x-axis shows the months since the Sargassum shock occurred, while the y-axis displays the size of the effect on nighttime light intensity. Thus, the blue line shows the size of the effect for each lag, and the grey area presents the 95% confidence interval (CI) around the estimated coefficient. Effects are considered to be significant when no area of the 95% CI coincides with the x-axis, here depicted as a red line. As can be observed, the effects of Sargassum detection appear to grow over time. In Figure 10, the negative trend grows larger over time during the first 5 months after Sargassum was detected, and the effect then stabilizes for months 6 to 12. The effect sizes appear to range between 0 and -1 nW/(cm^2·sr) for both regressions.

Figure 10: Effects of Sargassum detected on nighttime light intensity, 6-month lag

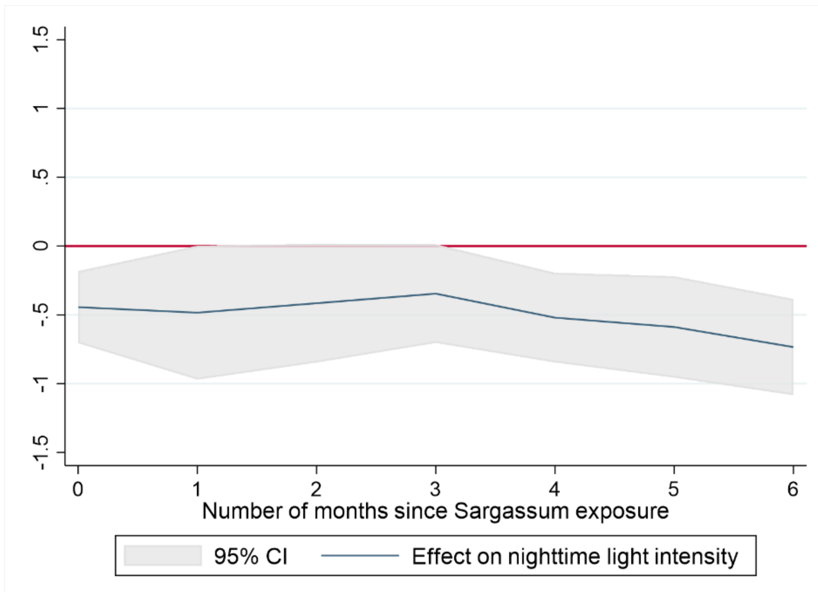

Figure 11: Effects of Sargassum detected on nighttime light intensity, 12-month lag

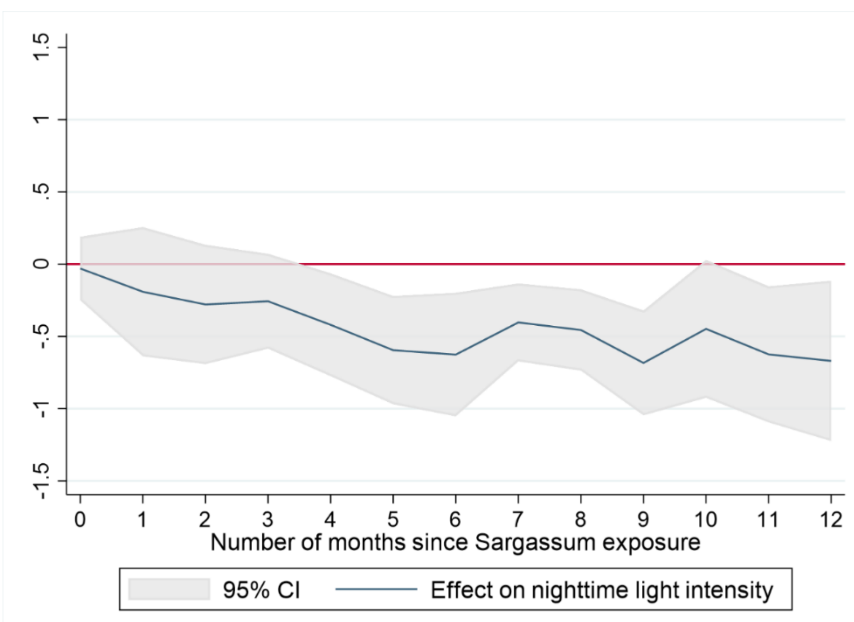

4.3 Robustness checks

Sargassum shock

As described in Section 2, there must be a considerably large amount of Sargassum in the beach segment for it to be detected by satellite imagery. Thus, it should not be too surprising that we observe effects of Sargassum detection on economic activity. Nevertheless, our remote measurement of Sargassum does not allow us to determine the exact volume of Sargassum washed ashore, so we cannot say with certainty that the detectable volume represents an unusual volume of algae at a given beach segment. One may argue that what would cause a drop in local economic activity as a result of less touristic activity and limitations to fishing and other shoreline activities, would be a Sargassum shock, meaning an unexpectedly large influx of Sargassum in a given month. Therefore, we consider a second measurement of Sargassum presence that captures the notion of such a shock, defined as a 1.5 standard deviation (SD) from the mean levels of Sargassum detected in each beach segment during the 4 years available in the dataset. We used the 1.5 SD threshold because it allowed us to exclude levels of Sargassum that could be considered "normal" for certain beach segments during the evaluated period. Although we could have used a stricter threshold, the 1.5 SD threshold already left us with only 9% of all month-beach segment combinations experiencing shocks. By design, the 1.5 SD threshold allows for most (98%) beach segments to experience a shock at least once.

Figure 12. Quarterly trend of Sargassum shocks

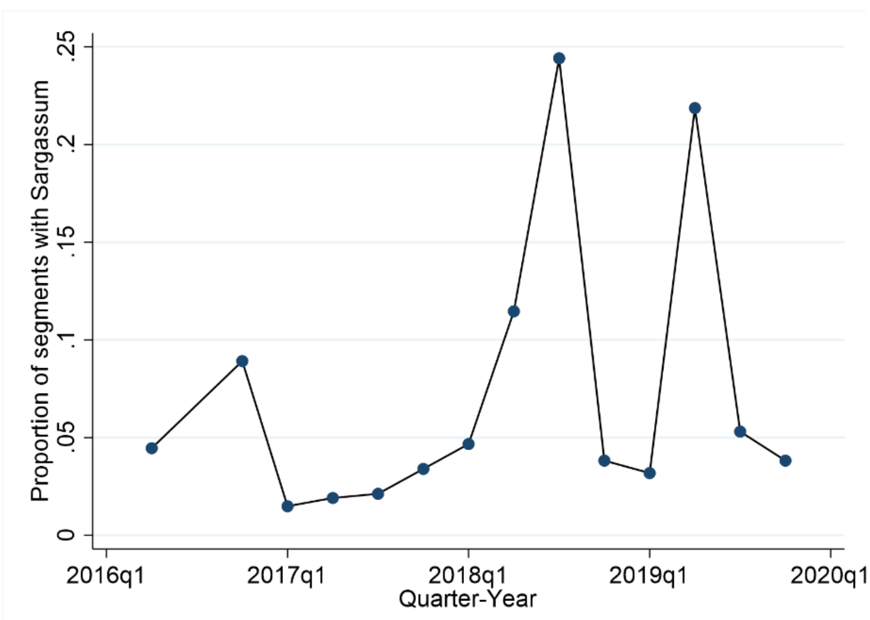

Figure 12 presents quarterly trends on the proportion of beach segments that experienced Sargassum shocks. As can be seen, the proportion of beach segments reporting such a shock is considerably smaller than the proportion of segments where Sargassum was detected (see Figure 6). However, the trend seems to be similar, and we find similar peaks in the first semester of 2018 and first quarter of 2019.

Table 10 reports results of the estimation with no lags (Model 1) when using the stricter definition of Sargassum shock. As can be observed in Column 1, we find an effect of 0.76 nW/(cm^2·sr) when controlling for time fixed effects only. When adding municipality-level fixed effects and beach segment controls in Column 2, a smaller but still significant effect of a decrease in 0.32 nW/(cm^2·sr) is found. However, this result becomes insignificant when adding clustered standard errors.

Table 10. Effects of a Sargassum shock on nighttime light intensity

Variables	**Nighttime light intensity** (1)	(2)	(3)
Sargassum shock (1.5 SD) in same month	**-0.759***** (0.278)	**-0.317*** (0.187)	-0.317 (0.213)
Time fixed effects	Yes	Yes	Yes
Segment-level controls		Yes	Yes
Municipality-level fixed effects		Yes	Yes
Municipality-level clustered standard errors			Yes
Number of observations	5,620	5,620	5,620
Adjusted R^2	0.254	0.739	0.739

Figures 12 and 13 show results for the most complete specification (including time fixed effects, municipality-level fixed effects, segment-level controls and municipality-level clustered standard errors) when including a 6-month lags and a 12-month lags, respectively. As can be observed in Figure 12, all effects are consistently negative, and we observe a significant negative effect in the 6th month after the shock occurred. In Figure 14 we also observe consistently negative effects, some of which are statistically significant beginning at month 6. On average, effect sizes range again between 0 and -1, though they appear slightly smaller than was found for general Sargassum presence.

Figure 13. Effects of Sargassum shock on nighttime light intensity, 6-month lag

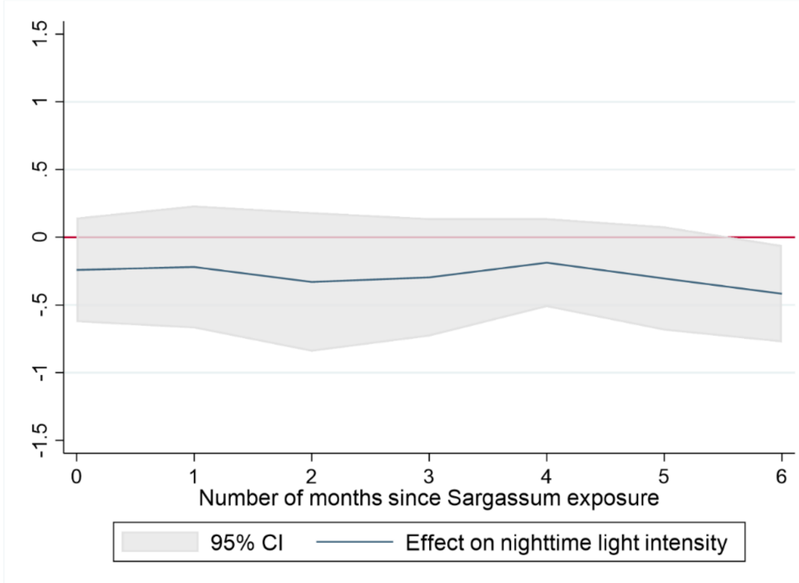

Figure 14. Effects of Sargassum shock on nighttime light intensity, 12-month lag

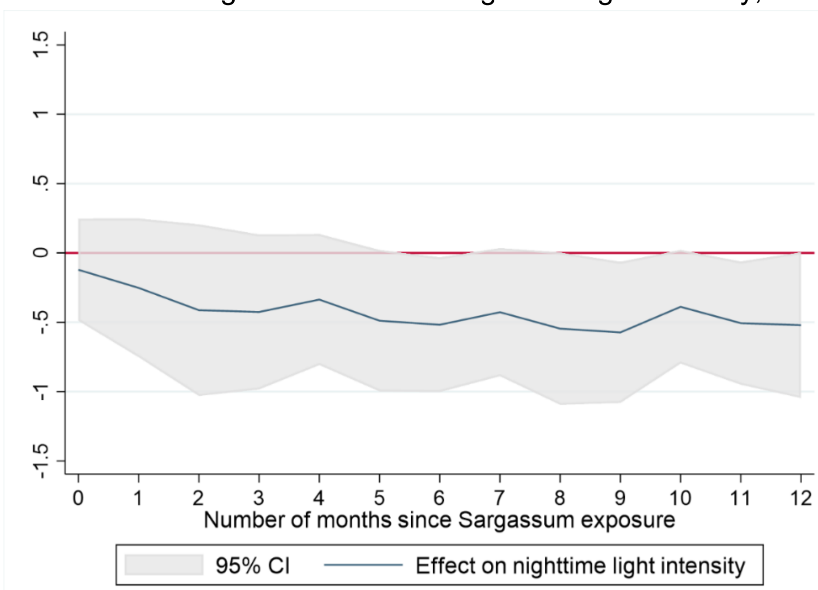

These results suggest that Sargassum has a negative effect on local economic activity, whether it be a detectable amount or a specific shock that exceeds average volume by 1.5 standard deviations. Since the initial definition of Sargassum presence seems to have more consistently negative and significant effects on nighttime light intensity, it would seem that a detectable amount of Sargassum is sufficient to drive away tourists and other economic activity, and it is not only the outlier events that cause economic harm.

Spatial correlation

Considering the potential for spatial correlation among neighboring beach segments, we repeat the analysis using Model (3). First, we analyze the effect of spatial correlation through a relationship between nighttime light intensity across neighboring beach segments, as described in model SAR-1. Figures 15 and 16 present the results of this estimation with 6- and 12-month time lags respectively. As observed in the main specification, estimated effects are consistently negative and become larger and size as well as increasingly statistically significant as time since Sargassum detection increases. Estimated effects by 12 months after Sargassum presence was detected lies at approximately 0.5 nW/($cm^2 \cdot sr$), which is equal to a 7% decrease in local economic activity when applying the estimated state-level GDP-nighttime light intensity elasticity.

Figure 15. Effects of Sargassum detected on nighttime light intensity with spatial correlation, 6-month lag (SAR-1)

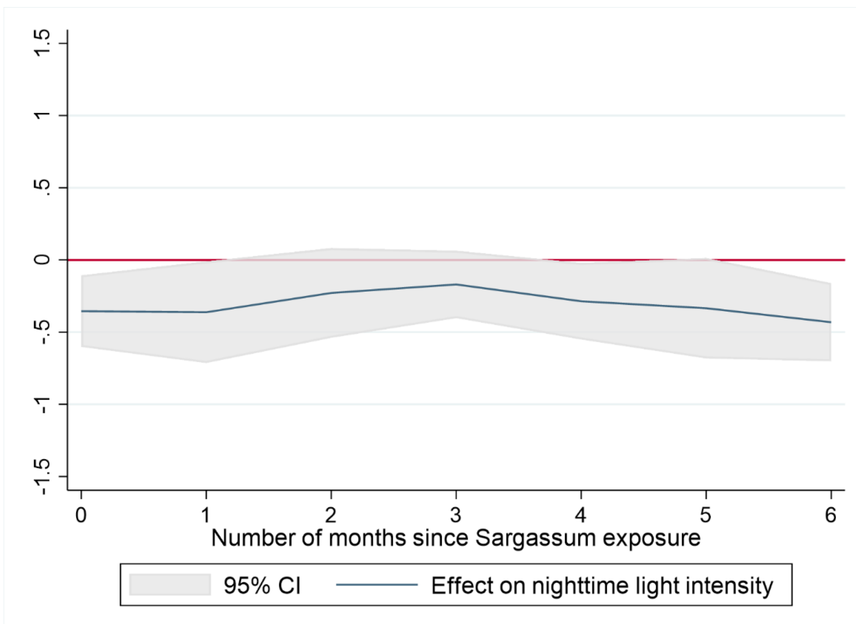

Figure 16. Effects of Sargassum on nighttime light intensity with spatial correlation, 12-months lag (SAR-1)

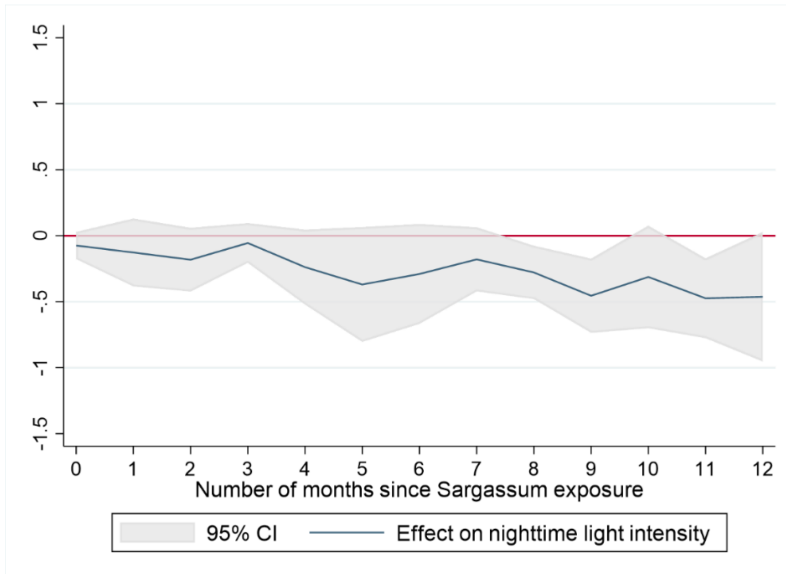

Figures 17 and 18 present results for our model SAR-2 which allows spatial correlation among neighboring beach segments to occur both through nighttime light intensity and Sargassum. The results under this model are again consistent with what we observed for previous models, with effect sizes being consistently negative and statistically significant. In this case, statistical significance is more consistently observed across all time lags, though effect sizes remain similar. In summary, controlling for spatial correlation highlights the robustness of estimated effects of Sargassum on nighttime light intensity.

Figure 17. Effects of Sargassum on nighttime light intensity with spatial correlation, 6-month lag (SAR-2)

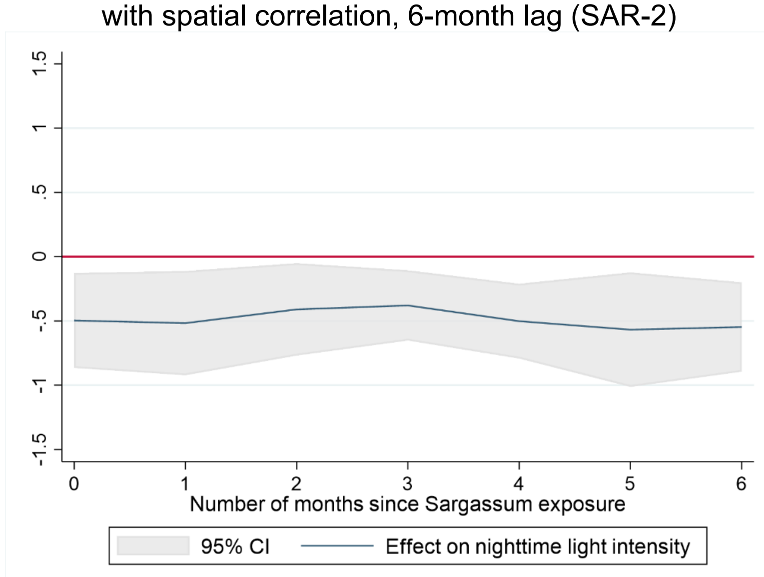

Figure 18. Effects of Sargassum on nighttime light intensity with Spatial correlation, 12-month lag (SAR-2)

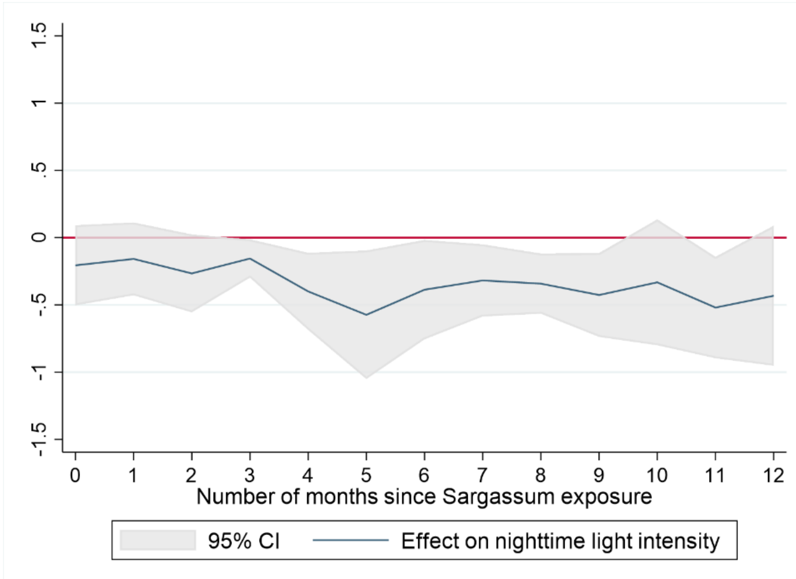

5 Conclusions

Latin America and the Caribbean has a wealth of coastal natural capital, and coastal areas are inextricably linked to the region's recent growth in both GDP and population, as coastal ecosystems support economies and communities with important goods and services, such as fisheries, tourism, and raw materials (Schueler, 2017).

For more than a decade, pelagic Sargassum has repeatedly washed ashore along the Caribbean and Gulf of Mexico coastlines in unprecedented quantities, covering whole beaches with seaweed and directly affecting businesses and local communities reliant on tourism and other economic activity within the region's popular coastal zone. The identified causes of these Sargassum blooms are increasingly high nutrient loads flushed out to sea from agriculture and poor land-use in both the Amazon and Congo River Basins and the Mississippi River, as well as rising ocean temperatures due to the effects of climate change (Huffard et al, 2014; Amaral-Zettler et al., 2016; Smetacek & Zingone, 2013; Johnson et al, 2013). While anecdotal evidence suggests that these unprecedented Sargassum events have led not only to a decline in economic revenue, but also to coastal erosion and economic losses in the traditional fishing industry, no rigorous analysis has yet been undertaken to quantify the causal effect on economic activity.

In this study, we attempt to fill this gap in empirical evidence by developing a unique dataset of 157 beach segments along the tourism-heavy shoreline of Quintana Roo State in Mexico that relies on a carefully designed geographic information systems (GIS) dataset, comprising extensive panel data on key infrastructure and beach characteristics, with four years (2016-2019) of monthly observations for influx of Sargassum seaweed, as well as remotely-sensed nighttime light intensity data as a proxy of economic growth. A novel time series of Sargassum distribution along beaches was created applying a machine learning algorithm to satellite imagery, and validation processes confirmed that the indicator is highly accurate in detecting Sargassum along the shoreline.

Applying a fixed-effects regression model that controls for general time trends and unobserved, time-invariant differences across observations, we estimate that the presence of Sargassum in a beach segment reduces nighttime light intensity by 17.5%, representing an approximate 11.6% decrease in gross local product. Taking into account that impacts of Sargassum on local economic activity may be delayed due to medium- and long-term reputational effects, our analysis finds that significant lagged effects can be detected up until 12 months after Sargassum was detected on the shoreline, with effect sizes ranging between a 5.9 and a 9.9% reduction in gross local product. Various robustness checks, including an adjusted measurement of Sargassum and the consideration of potential spatial correlation across beach segments, indicate that estimated impacts are consistently significant and negative across numerous specifications. Overall, we can conclude that Sargassum is a relevant concern that significantly affects local economies that rely on tourism. Therefore, it seems important not only to find ways to respond to the unwanted presence of Sargassum, but also to address the main factors contributing to the increasing growth of algae blooms, such as high nutrient loads that are caused by unsustainable agricultural practices.

This analysis is unable to establish with empirical evidence the theoretical channels of impact through the tourism and fishery industry, amongst other potential causal pathways. As we highlight, nighttime light intensity can only serve as a proxy measure for local economic activity and does not allow us to tease out whether reduced radiance is caused by a decrease in hotel occupancy or restaurant visits, for instance. Future research in this vein should provide a deeper understanding of how tourists react to the presence of Sargassum algae along the beach stretch where they planned to spend their vacation, and how it affects the present and future travel choices. This would allow policy makers to better assess the potential economic consequences of massive Sargassum inflow and determine what would constitute a reasonable cost of Sargassum cleanup to offset potential economic losses.

Appendix

A. Additional Tables and Figures

Table AI. Elasticity of GDP with regards to nighttime light intensity [a]

	Log of Quintana Roo GDP
Log of nighttime light intensity	**0.66** ***
	(0.126)
Constant	-0.54
	(1.020)
Observations	20

[a] Difference unequal to zero if p-value significant at the 99 (***), 95 (**), or 90 (*) confidence level. Standard errors reported in parentheses.

References

Administración Portuaria Integral de Quintana Roo (APIQROO, 2021). Portal de Estadísticas. Retrieved on December 22, 2021 from http://servicios.apiqroo.com.mx/estadistica/index.php

Agnew, J., Gillespie, T. W., Gonzalez, J., & Min, B. (2008). Baghdad nights: Evaluating the US military 'surge' using nighttime light signatures. *Environment and Planning A*, 40(10), 2285-2295. doi: 10.1068/a41200

Alesina, A., Michalopoulos, S., Papaioannou, E. (2016). Ethnic inequality. *Journal of Political Economy*, 124(2), 428–488. doi: 10.1086/685300

Amaral-Zettler, L. A., Dragone, N. B., Schell, J., Slikas, B., Murphy, L. G., Morrall, C. E., & Zettler, E. R. (2017). Comparative Mitochondrial and Chloroplast Genomics of a Genetically Distinct Form of Sargassum Contributing to Recent "Golden Tides" in the Western Atlantic. *Ecology and Evolution*, 7(2), 516-525. doi: 10.1002/ece3.2630

Ángeles, M. del R. & Sánchez, A. (2017). Huracán 'Irma' deja toneladas de sargazo en playas de Q. Roo. Retrieved on December 22, 2021 from https://noticieros.televisa.com/ultimas-noticias/huracan-irma-dejo-sargazo-playas-q-roo/

Avtar, R., Aggarwal, R., Kharrazi, A., Kumar, P., & Kurniawan, T. A. (2020). Utilizing geospatial information to implement SDGs and monitor their progress. *Environmental Monitoring and Assessment*, 192, 1-12. doi: 10.1007/s10661-019-7996-9

Azuz-Adeath, I., & Rivera, E. (2019). Current Demographic Conditions and Future Scenarios in Mexico's Coastal Zone. *Revisata de Gestão Costeira Integrada,* 19(2), 85-122, doi: 10.5894/rgci-n216

Bennett, D. C., & Sharpe, K. F. (1985). *Transnational Corporations versus the State: The Political Economy of the Mexican Automobile Industry*. Princeton, N.J.: Princeton University Press.

Breiman, L. (2001). Random Forests. *Machine Learning*, 45(1), 5–32. doi: 10.1023/A:1010933404324

Burrowes, R., Wabnitz, C., & Eyzaguirre, J. (2019). The Great Sargassum Disaster of 2018. ESSA Technologies Ltd. Available at: https://essa.com/the-great-sargassum-disaster-of-2018

Cabanillas-Teran, N., Hernandez-Arana, H. A., Ruiz-Zarate, M.-A., Vega-Zepeda, A., & Sanchez-Gonzalez, A. (2019). Sargassum blooms in the Caribbean alter the trophic structure of the sea urchin Diadema antillarum. *Peerj*, 2019(8). doi: 10.7717/peerj.7589

Cao, C. & Bai, Y. (2014). Quantitative analysis of VIIRS DNB nightlight point source for light power estimation and stability monitoring. *Remote Sensing*, 6(12), 11915-11935. doi: 10.3390/rs61211915

Cauwels, P., Pestalozzi, N., & Sornette, D. (2014). Dynamics and spatial distribution of global nighttime lights. *EPJ Data Science*, 3(1), 2-27. doi: 10.1140/epjds19

Chávez, V., Uribe-Martínez, A., Cuevas, E., Rodríguez-Martínez, R. E., van Tussenbroek, B. I., Francisco, V., Estévez, M., Celis, L. B., Monroy-Velázquez, L. V., Leal-Bautista, R., Álvarez-Filip, L., García-Sánchez, M., Masia, L., & Silva, R. (2020). Massive Influx of Pelagic

Sargassum spp. on the Coasts of the Mexican Caribbean 2014–2020: Challenges and Opportunities. *Water*, 12(10), 2908. doi: 10.3390/w12102908

Clancy, M. (2001). Mexican Tourism: Export Growth and Structural Change since 1970. *Latin American Research Review,* 36(1), 128-150. http://www.jstor.org/stable/2692077

Coesfeld, J., Kuester, T., Kuechly, H. U., & Kyba, C. C. M. (2020). Reducing Variability and Removing Natural Light from Nighttime Satellite Imagery: A Case Study Using the VIIRS DNB. *Sensors*, 20(11), 3287. doi: 10.3390/s20113287

Comisión Nacional de Acuacultura y Pesca (CONAPESCA, 2012). *Anuario Estadístico de Acuacultura y Pesca 2012.* Mazatlán: CONAPESCA.

Comisión Nacional para el Conocimiento y Uso de la Biodiversidad (CONABIO). (2019). CONABIO genera nueva cartografía de la línea de costa de México. Retrieved on December 21, 2021 from https://www.gob.mx/conabio/prensa/conabio-genera-nueva-cartografia-de-la-linea-de-costa-de-mexico?idiom=es

Corral, L. R. & Schling, M. (2017). The impact of shoreline stabilization on economic growth in small island developing states. *Journal of Environmental Economics and Management*, 86, 210-228. doi: 10.1016/j.jeem.2017.06.001

Corral, L. R., Schling, M., Montiel, C. (2018). *The economic and ecological impact of natural resource extraction – The case of the Camisea gas project in Peru*. (IDB Working Paper Series No. IDB-WP-00934). Washington, DC: Inter-American Development Bank. doi: 10.18235/0001315

Cruz, C., Mendoza, E., Silva, R., & Chávez, V. (2019). Assessing degrees of anthropization on the coast of Mexico from ecosystem conservation and population growth data. *Journal of Coastal Research*, 92(sp1), 136-144. doi: 10.2112/SI92-016.1

Cuevas, E., Uribe-Martínez, A., & Liceaga-Correa, M. de los Á. (2018). A satellite remote-sensing multi-index approach to discriminate pelagic Sargassum in the waters of the Yucatan Peninsula, Mexico. *International Journal of Remote Sensing*, 39(11), 3608–3627. doi: 10.1080/01431161.2018.1447162

Dell, M., Jones, B. F., & Olken, B. A. (2009). Temperature and income: reconciling new cross-sectional and panel estimates. *American Economic Review*, 99(2), 198-204.

Deschênes, O., & Greenstone, M. (2007). The economic impacts of climate change: evidence from agricultural output and random fluctuations in weather. *American Economic Review*, 97(1), 354-385.

Earth Observation Group (EOG, 2021). VIIRS Nighttime Light. *National Oceanic and Atmospheric Administration (NOAA*). Retrieved from https://eogdata.mines.edu/products/vnl/ (Accessed April 8, 2021).

Elvidge, C.D., Baugh, K.E., Kihn, E.A., Kroehl, H.W & Davis, E.R. (1997). Mapping of city lights using DMSP Operational Linescan System data. *Photogrammetric Engineering and Remote Sensing*, 63, 727-734. Retrieved from http://www.csiss.org/SPACE/workshops/2006/OU/docs/Elvidge_et_al_1997a_001.pdf (Accessed April 6, 2021).

Elvidge, C.D., Baugh, K.E., Zhizhin,M., Hsu, F. C., & Ghosh, T. (2017). VIIRS night-time lights. *International Journal of Remote Sensing*, 38(21), 5860-5879. doi: 10.1080/01431161.2017.1342050

Espinosa, L. A., & Li Ng, J. J. (2020). The Risk of Sargassum to the Economy and Tourism of Quintana Roo and Mexico. Working Paper 20/02. Mexico City: BBVA Research.

Felbermayr, G., Gröschl, J., Sanders, M., Schippers, V., & Steinwachs, T. (2022). The economic impact of weather anomalies. *World Development*, 151, 105745.

Fisher, A. C., Hanemann, W. M., Roberts, M. J., & Schlenker, W. (2012). The economic impacts of climate change: evidence from agricultural output and random fluctuations in weather: comment. *American Economic Review*, 102(7), 3749-60.

Food and Agricultural Organization (FAO, 2017). "Climate change adaptation in the eastern Caribbean fisheries sector launching workshop", Western Central Atlantic Fishery Commission, FAO Fisheries and Acquaculture Report SLC/FIA R1189. FAO: Rome, Italy. Available at: https://www.fao.org/3/i8281en/I8281EN.pdf

Franks, J. S., Johnson, D. R., & Ko, D. S. (2016). Pelagic Sargassum in the Tropical North Atlantic. *Gulf and Caribbean Research*, 27(1), SC6-SC11. doi: 10.18785/gcr.2701.08

Gavio, B., & Santos-Martinez, A. (2018). Floating sargassum in Serranilla Bank, Caribbean Colombia, may jeopardize the race to the ocean of baby sea turtles. *Acta Biológica Colombiana*, 23(3), 311–313. doi: 10.15446/abc.v23n3.68113

Ghosh, T., Powell, R., Elvidge, C. D., Baugh, K. E., Sutton, P. C., & Anderson, S. (2010). Shedding light on the global distribution of economic activity. *The Open Geography Journal*, 3, 148–161. doi: 10.2174/1874923201003010147

Google Earth Engine (GEE, 2021). *VIIRS Nighttime Day/Night Band Composites Version 1*. Available at: https://developers.google.com/earth-engine/datasets/catalog/NOAA_VIIRS_DNB_MONTHLY_V1_VCMCFG

Gorelick, N., Hancher, M., Dixon, M., Ilyushchenko, S., Thau, D., & Moore, R. (2017). Google Earth Engine: Planetary-scale geospatial analysis for everyone. *Remote Sensing of Environment*, 202, 18–27. doi: 10.1016/j.rse.2017.06.031

Government of Mexico. (2015). Continúan acciones de limpieza de sargazo en 180km de playas en Quintana Roo. Retrieved on December 22, 2021 from https://www.gob.mx/epn/es/articulos/continuan-acciones-de-limpieza-de-sargazo-en-180-km-de-playas-en-quintana-roo

Government of Quintana Roo. (2019). Mensaje del Gobernador Carlos Joaquín en el Primer Encuentro de Alto Nivel para la Atención del Sargazo en el Mar Caribe. Retrieved on December 22, 2021 from http://cgc.qroo.gob.mx/mensaje-del-gobernador-carlos-joaquin-en-el-primer-encuentro-de-alto-nivel-para-la-atencion-del-sargazo-en-el-mar-caribe/

Gower, J., Hu, C., Borstad, G., & King, S. (2006). Ocean color satellites show extensive lines of floating Sargassum in the Gulf of Mexico. *IEEE Transactions on Geoscience and Remote Sensing*, 44 (12), 3619–3625. doi: 10.1109/TGRS.2006.882258

Gower, J., Young E., & S. King. (2013). Satellite Images Suggest a New Sargassum Source Region in 2011. *Remote Sensing Letters* 4:764—773. doi: 10.1080/2150704X.2013.796433

Greene, W. H. (2002). *Econometric Analysis* (5th ed.). Upper Saddle River, NJ: Prentice Hall.

Guerrero Compeán, R. (2013). Climate Shocks, Safety Nets and Shielded Poor: Experimental Evidence from Rural Mexico. In Guerrero Compeán, R. *Essays in Climate and Development.* Cambridge, MA: Massachusetts Institute of Technology.

Hallegatte, S. (2005). The long time scales of the climate–economy feedback and the climatic cost of growth. *Environmental Modeling & Assessment*, 10(4), 277-289.

Hanisak, M. D., & Samuel, M.A. (1987). Growth Rates in Culture of Several Species of *Sargassum* from Florida, USA, in Ragan, M. A. & Bird, C. J. (eds.) *Proceedings of the Twelfth International Seaweed Symposium,* pp. 399-404. doi: 10.1007/978-94-009-4057-4_59

Hausman, J.A. (1978). Specification tests in econometrics. *Econometrica*, 46(6), 1251-1271. doi: 10.2307/1913827

Henderson, J. V., Storeygard, A., & Weil, D. N. (2012). Measuring economic growth from outer space. *American Economic Review*, 102(2), 994-1028. doi: 10.1257/aer.102.2.994

Hu, C. (2009). A novel ocean color index to detect floating algae in the global oceans. *Remote Sensing of Environment*, 113(10), 2118-2129. doi: 10.1016/j.rse.2009.05.012

Hu, C., Feng, L., Hardy, R., & Hochberg, E. (2015). Spectral and spatial requirements of remote measurements of pelagic Sargassum macroalgae. *Remote Sensing of Environment*, 167, 229-246. doi: 10.1016/j.rse.2015.05.022

Huffard, C. L., von Thun, S., Sherman, A. D., Sealey, K., & Smith Jr., K. L. (2014). Pelagic Sargassum Community Change over a 40-year Period: Temporal and Spatial Variability. *Marine Biology* 161, 2735–2751. doi: 10.1007/s00227-014-2539-y

Institute of Statistics and Geography of Mexico (INEGI, 2021). *PIB por entidad federative (PIBE). Base 2013.* Retrieved on December 22, 2021 from https://www.inegi.org.mx/programas/pibent/2013/#Tabulados

Institute of Statistics and Geography of Mexico (INEGI, 2020). National Statistical Directory of Economic Units (DENUE). Retrieved on November 11, 2021 from https://www.inegi.org.mx/app/mapa/denue/default.aspx

Institute of Statistics and Geography of Mexico (INEGI, 2019). Economic Information Databank. Retrieved on December 21, 2021 from https://inegi.org.mx/app/indicadores/?tm=0&ind=473488#divFV487582#D473488

Institute of Statistics and Geography of Mexico (INEGI, 2015). *Principales resultados de la Encuesta Intercensal 2015: Quintana Roo.* Mexico City: INEGI. 92 p.

Inter-American Development Bank (IDB, 1972). *Annual Report, 1971*. Washington, D.C.: IDB.

Ivan, K., Holobâcam I., Benedek, J., & Török, I. (2020). VIIRS nighttime light data for income estimation at local level. *Remote Sensing*, 12(18), 2950. doi: 10.3390/rs12182950

Jing, X., Shao, X., Cao, C., Fu, X., & Yan, L. (2016). Comparison between the Suomi-NPP day-night band and DMSP-OLS for correlating socio-economic variables at the provincial level in China. *Remote Sensing*, 8(1), 17. doi: 10.3390/rs8010017

Johnson, D. R., Ko, D. S., Franks, J. S., Moreno, P., & Sánchez-Rubio, G. (2013). The Sargassum Invasion of the Eastern Caribbean and Dynamics of the Equatorial North Atlantic. *Proceedings of the 65th Gulf and Caribbean Fisheries Institute.* November 5-9, 2012, Santa Marta, Colombia.

Kyba, C., Kuester, T., Sánchez de Miguel, A., Baugh, K., Jechow, A., Hölker, F., ... & Guanter, L. (2017). Artificially lit surface of earth at night increasing in radiance and extent. *Science Advances,* 3, e1701528. doi: 10.1126/sciadv.1701528

León, C. (2004). Piezas de un rompecabezas: Dimensión socioeconómica de las costas de México in Rivero Arriaga, E., Villalobos, G.J, Azuz Adeath, I., & Rosado May, F. (eds.) *El manejo costero en México.* Universidad Autónoma de Campecha, SEMARNAT, CETYS-Universidad, Universidad de Quintana Roo, pp. 5-26.

Levin, N., Kyba, C., Zhang, Q., Sánchez de Miguel, A., Román, M. O., Li, X., ..., & Elvidge, C. (2020). Remote sensing of night lights: A review and an outlook for the future. *Remote Sensing of Environment*, 237, 111443. doi: 10.1016/j.rse.2019.111443

Louime, C., Fortune, J., & Gervais, G. (2017). Sargassum Invasion of Coastal Environments: A Growing Concern. *American Journal of Environmental Sciences*, 13(1), 58-64. doi: 10.3844/ajessp.2017.58.64

Maddison, D., & Rehdanz, K. (2011). The impact of climate on life satisfaction. *Ecological Economics*, 70(12), 2437-2445.

Maldonado, J. H.; Moreno Sánchez, R.; Vargas Morales, M. E.; Henao Henao, J. P.; González Tarazona, Y.; Guerrero Compeán, R.; Schling, M. (2020). "Innovation in Economic Analysis and Evaluation Approaches for Coastal Protection and Restoration Investments in the Caribbean", Inter-American Development Bank Technical Note IDB-TN-01861. IDB: Washington, DC. Available at: http://dx.doi.org/10.18235/0002184

Méndez Tejeda, R., & Rosado Jiménez, G. A. (2019). Influence of Climatic Factors on Sargassum Arrivals to the Coasts of the Dominican Republic. *Journal of Oceanography and Marine Science*, 10(2), 22-32. doi: 10.5897/JOMS2019.0156

Miguel, A. S. de, Kyba, C. C. M., Zamorano, J., Gallego, J., & Gaston, K. J. (2020). The nature of the diffuse light near cities detected in nighttime satellite imagery. *Scientific Reports*, *10*(1), 1–16. doi: 10.1038/s41598-020-64673-2

Ministry of Tourism of Mexico. (2020). Estadística Turística Derivada de los Censos Económicos 2019. Dirección General de Integración de Información Sectorial. Retrieved on December 22, 2021 from https://www.datatur.sectur.gob.mx/Comite%20de%20Estadisticas%20del%20Sector%20Turismo/Turismo_Censos_19_General.pdf

Ministry of Tourism of Quintana Roo. (2019). Indicadores turísticos enero-diciembre 2019. Retrieved on December 21, 2021 from https://sedeturqroo.gob.mx/ARCHIVOS/indicadores/Indicador-Tur-Dic-2019.pdf

Moulton, B.R. (1986). Random group effects and the precision of regression estimates. *Journal of Econometrics*, 32, 385-397. doi: 10.1016/0304-4076(86)90021-7

National Oceanic and Atmospheric Administration (NOAA, 2019). *Sargassum density and coverage using Moderate Resolution Imaging Spectroradiometer (MODIS) satellite data from 2001-01-01 to 2018-12-31 (NCEI Accession 0190272).* Retrieved from https://accession.nodc.noaa.gov/0190272 (Accessed April 20, 2021).

Oviatt, C. A., Huizenga, K., Rogers, C. S., & Miller, W. J. (2019). What nutrient sources support anomalous growth and the recent sargassum mass stranding on Caribbean beaches? A review. *Marine Pollution Bulletin*, 145, 517–525. doi: 10.1016/j.marpolbul.2019.06.049

Porter, J. R., Xie, L., Challinor, A. J., Cochrane, K., Howden, S. M., Iqbal, M. M., Lobell, D. B. & Travasso, M. I. (2014). Food security and food production systems. In *Climate Change 2014: Impacts, Adaptation, and Vulnerability. Part A: Global and Sectoral Aspects. Contribution of Working Group II to the Fifth Assessment Report of the Intergovernmental Panel on Climate Change*, ed. C. B. Field, V. R. Barros, D. J. Dokken, K. J. Mach, M. D. Mastrandrea, T. E. Bilir, M. Chatterjee, K. L. Ebi, Y. O. Estrada, R. C. Genova, B. Girma, E. S. Kissel, A. N. Levy, S. MacCracken, P. R. Mastrandrea, and L. L. White, 659–708. Cambridge: Cambridge University Press.

Putman, N. F., Goni, G. J., Gramer, L. J., Hu, C., Johns, E. M., Trinanes, J., & Wang, M. (2018). Simulating transport pathways of pelagic Sargassum from the equatorial atlantic into the Caribbean Sea. *Progress in Oceanography*, 165, 205–214. doi: 10.1016/j.pocean.2018.06.009

Ramlogan, N. R., McConney, P., & Oxenford, H. A. (2017). Socio-economic Impacts of Sargassum Influx Events on the Fishery Sector of Barbados. Centre for Resource Management and Environmental Studies (CERMES) Technical Report No 81.

Reguero, B. G., Secaira, F., Toimil, A., Escudero, M., Díaz-Simal, P., Beck, M. W., ... Losada, I. J. (2019). The risk reduction benefits of the Mesoamerican reef in Mexico. *Frontiers in Earth Science*, *7*. doi: 10.3389/feart.2019.00125

Robledo, D. & Vázquez-Delfín, É. (2019). Sargazo, conociendo al “enemigo”. *Avance y Perspectiva* 5(3).

Rodríguez Martínez, R. E., van Tussenbroek, B., Jordán-Dahlgren, E. (2016). *Afluencia masiva de sargazo pelágico a la costa del Caribe mexicano (2014-2015).* Puerto Morelos, Quintana Roo: Universidad Nacional Autónoma de México, Instituto de Ciencias del Mar y Limnología.

Schell, J. M., Goodwin, D. S., & Siuda, A. N. (2015). Recent Sargassum Inundation Events in the Caribbean: Shipboard Observations Reveal Dominance of a Previously Rare Form. *Oceanography*, 28(3), 8-11. https://www.jstor.org/stable/24861895

Schueler, K. (2017). *Nature-Based Solutions to Enhance Coastal Resilience.* Washington, D.C.: Inter-American Development Bank.

Sharp, R., Douglass, J., Wolny, S., Arkema, K., Bernhardt, J., Bierbower, W., … Wyatt, K. (2020). *InVEST 3.9.0.post159+ug.g367dd89 User's Guide.* The Natural Capital Project, Stanford University, University of Minnesota, The Nature Conservancy, and World Wildlife Fund. Retrieved from http://releases.naturalcapitalproject.org/invest-userguide/latest/ (Accessed April 20, 2021).

Smetacek, V., & Zingone, A. (2013). Green and Golden Seaweed Tides on the Rise. *Nature*, 504(7478), 84-88. doi: 10.1038/nature12860

Solarin, B. B., Bolaji, D. A., Fakayode, O. S., & Akinnigbagbe, R. O. (2014). Impacts of an Invasive Seaweed *Sargassum hystrix var. fluitans* (Børgesen 1914) on the Fisheries and Other Economic Implications for the Nigerian Coastal Waters. *IOSR Journal of Agriculture and Veterinary Science*, 7(7), 1-6.

Stock, J. H., & Watson, M. W. (2011). *Introduction to Econometrics* (3rd ed.). Boston, MA: Addison-Wesley.

Storeygard, A. (2013). *Farther on down the road: Transport costs, trade and urban growth in sub-Saharan Africa* (Policy Research Working Paper No. 6444). Washington, DC: The World Bank. doi: 10.1093/restud/rdw020

Sutton, P. C. & Costanza, R. (2002). Global estimates of market and non-market values derived from nighttime satellite imagery, land cover, and ecosystem service valuation. *Ecological Economics*, 41(3), 509-527. doi: 10.1016/S0921-8009(02)00097-6

Tol, R. S. (2020). The economic impacts of climate change. *Review of Environmental Economics and Policy* 12(1).

Torres, R.M., & Momsen, J.D. (2005). Gringolandia: The Construction of a New Tourist Space in Mexico. *Annals of the Association of American Geographers,* 95(2), 314-335. doi: 10.1111/j.1467-8306.2005.00462.x

United Nations Environment Programme-Caribbean Environment Programme (UNEP-CEP, 2021). *Sargassum White Paper. Turning the Crisis into an Opportunity.* Ninth Meeting of the Scientific and Technical Advisory Committee (STAC) to the Protocol Concerning Specially Protected Areas and Wildlife (SPAW) in the Wider Caribbean Region. Kingston, Jamaica.

van Tussenbroek, B. I., Hernández Arana, H. A., Rodríguez-Martínez, R. E., Espinoza-Avalos, J., Canizales-Flores, H. M., González-Godoy, C. E., Barba-Santos, M. G., Vega-Zepeda, A., & Collado-Vides, L. (2017). Severe impacts of brown tides caused by sargassum spp. on near-shore Caribbean seagrass communities. *Marine Pollution Bulletin*, 122(1-2), 272–281. doi: 10.1016/j.marpolbul.2017.06.057

Wang, M., & Hu, C. (2016). Mapping and quantifying Sargassum distribution and coverage in the Central West Atlantic using MODIS observations. *Remote Sensing of Environment*, 183, 350-367. doi: 10.1016/j.rse.2016.04.019

Wang, M., Hu, C., Barnes, B., Mitchum, G., Lapointe, B., & Montoya, J. (2019). The great Atlantic Sargassum belt. *Science*, 365(6448), 83-87. doi: 10.1126/science.aaw7912

Williams, A., & Feagin, R. (2010). Sargassum as a natural solution to enhance dune plant growth. *Environmental Management*, 46(5), 738-747. doi: 10.1007/s00267-010-9558-3

WorldPop (2020). *Mapping Populations.* Retrieved from https://www.worldpop.org/methods/populations (Accessed November 11, 2020).

World Travel & Tourism Council (WTTC, 2018). *City Travel & Tourism Impact 2018.* London: WTTC.